REPORT DOCUMENTATION PAGE

Form Approved
OMB NO. 0704-0188

1. AGENCY USE ONLY (Leave Blank)	2. REPORT DATE 31 March 2000	3. REPORT TYPE AND DATES COVERED Final Report

4. TITLE AND SUBTITLE

Experimental Study of Metal Corrosion in Supercritical Brines: Application to Supercritical Water Oxidation of Hazardous Wastes

5. FUNDING NUMBERS

DAAH04-96-1-0395

6. AUTHOR(S)
Scott A. Wood and Leslie L. Baker

7. PERFORMING ORGANIZATION NAME(S) AND ADDRESS(ES)

University of Idaho
Moscow, ID 83843

8. PERFORMING ORGANIZATION REPORT NUMBER

9. SPONSORING / MONITORING AGENCY NAME(S) AND ADDRESS(ES)

U. S. Army Research Office
P.O. Box 12211
Research Triangle Park, NC 27709-2211

10. SPONSORING / MONITORING AGENCY REPORT NUMBER

ARO 36324.1-CH-DPS

11. SUPPLEMENTARY NOTES
The views, opinions and/or findings contained in this report are those of the author(s) and should not be construed as an official Department of the Army position, policy or decision, unless so designated by other documentation.

12 a. DISTRIBUTION / AVAILABILITY STATEMENT

Approved for public release; distribution unlimited.

12 b. DISTRIBUTION CODE

13. ABSTRACT The corrosion behavior of Hastelloy C, titanium, zirconium, niobium, tantalum, and gold have been studied as a function of temperature (200° - 400°C), acid concentration (0 - 0.02 mol/Kg), oxygen content (0.1-1 mol %) and NaCl content (0 - 0.2 mol/Kg). The intent of these experiments was to determine an empirical rate law for corrosion of these metals as a function of the parameters listed above. Due to the complexity of the corrosion behavior of these metals and the different responses of different metals, rate law determination was not possible. However, our results qualitatively indicate that Nb and Zr are not suitable for service under SCWO conditions, for they rapidly convert to oxides which erode into the fluid. Ti proved resistant to dissolution into the fluids, but was subject to pitting corrosion. Au was subject to galvanic effects, which increased its dissolution rate. This suggests that gold would not be suitable for use with other metals in a SCWO system. Stainless steel and Hastelloy C displayed fairly rapid corrosion, with Ni and Mn preferentially dissolving out of the metal and Cr and Mo remaining behind. Tantalum proved to be the most resistant metal tested, and is an excellent candidate for possible long-term use under highly corrosive conditions.

14. SUBJECT TERMS

15. NUMBER OF PAGES

20000707 154

16. PRICE CODE

17. SECURITY CLASSIFICATION OR REPORT UNCLASSIFIED	18. SECURITY CLASSIFICATION ON THIS PAGE UNCLASSIFIED	19. SECURITY CLASSIFICATION OF ABSTRACT UNCLASSIFIED	20. LIMITATION OF ABSTRACT UL

NSN 7540-01-280-5500

DTIC QUALITY INSPECTED 4

Standard Form 298 (Rev.2-89)
Prescribed by ANSI Std. 239-18
298-102

1) No manuscripts have been published or submitted from this work.

2) List of scientific personnel supported : see Page 28

3) No inventions have resulted from this work.

4) Scientific progress and accomplishments: see attached

5) No technology transfer activities have taken place as a result of this work.

EXPERIMENTAL STUDY OF METAL CORROSION IN SUPERCRITICAL
BRINES: APPLICATION TO SUPERCRITICAL WATER OXIDATION
OF HAZARDOUS WASTES

FINAL REPORT

LESLIE L. BAKER AND SCOTT A. WOOD

31 MARCH 2000

U.S. ARMY RESEARCH OFFICE

GRANT NUMBER DAAH04 - 96 - 1 - 0395

DEPARTMENT OF GEOLOGY AND GEOLOGICAL ENGINEERING
UNIVERSITY OF IDAHO
MOSCOW, IDAHO

APPROVED FOR PUBLIC RELEASE;

DISTRIBUTION UNLIMITED

EXPERIMENTAL STUDY OF METAL CORROSION IN SUPERCRITICAL BRINES: APPLICATION TO SUPERCRITICAL WATER OXIDATION OF HAZARDOUS WASTES

TABLE OF CONTENTS

ABSTRACT

The environmentally sound disposal of hazardous chemicals, including chemical weapons, outdated explosives, propellants, dyes, smokes and pyrotechnics, and human waste (e.g., from ships) is of great concern to the U.S. Armed Forces. A promising technology being considered for this task is the combustion of these chemicals under high pressure and at high temperature in a supercritical aqueous fluid phase, i.e., SuperCritical Water Oxidation (SCWO) or HydroThermal Oxidation (HTO). For many substances that have been tested, the breakdown of the hazardous wastes to relatively innocuous compounds such as H_2O, CO_2 and N_2 is better than 99.9% complete at relatively low temperatures (400° to 600°C), unlike conventional incineration or wet combustion. However, SCWO treatment of many DoD wastes containing S, Cl, F, and P result in the production of strongly acidic fluids with high salt content. These fluids present the challenge of finding sufficiently corrosion-resistant materials for the construction of SCWO reactors. Few data are currently available on the performance of various metals and metal alloys in corrosive SCWO environments.

The corrosion behavior of Hastelloy C, titanium, zirconium, niobium, tantalum, and gold have been studied as a function of temperature (200° - 400°C), acid concentration (0 - 0.02 mol/Kg), oxygen concentration (0.1-1 mol %) and NaCl content (0 - 0.2 mol/Kg). The intent of these experiments was to determine an empirical rate law for corrosion of these metals as a function of the parameters listed above. Due to the complexity of the corrosion behavior of these metals and the different responses of different metals, rate law determination was not possible. However, our results qualitatively indicate that niobium and zirconium are not suitable for service under SCWO conditions, for they rapidly covert to oxides which erode into the fluid. Titanium proved resistant to dissolution into the fluids, but was subject to pitting corrosion. Gold was subject to galvanic effects, dissolving in the experimental fluid and recrystallizing on the surfaces of other metals such as Ti, Ta, and Hastelloy. This suggests that gold would not be suitable for use with other metals in a SCWO system. Stainless steel and Hastelloy C displayed fairly rapid corrosion, with Ni and Mn preferentially dissolving out of the metal and into the fluid, and Cr and Mo remaining behind. Tantalum proved to be the most resistant metal tested, and is an excellent candidate for possible long-term use under highly corrosive conditions.

INTRODUCTION

The Department of Defense generates enormous amounts of hazardous and human wastes from normal daily operations. For example, the Navy alone generates 2,500,000 gal/yr of liquid hazardous wastes (Marsh, 1995). In addition, large stockpiles of obsolete fuels, explosives, chemical warfare agents, smokes and dyes must be safely disposed of by the Army, the Navy and the Air Force. In a number of cases, base closings require the remediation of sites contaminated with hazardous wastes prior to their return to civilian use. A very promising means of disposing of these wastes is known as supercritical waste oxidation (SCWO), also referred to as hydrothermal oxidation (HTO) (see Shaw et al., 1991; Barner et al., 1992; Tester et al., 1993 for reviews of HTO). In SCWO, hazardous organic materials are heated with oxygen in an aqueous fluid to temperatures and pressures above the critical point (for pure water, 374°C and 221 bars), whereby the waste is oxidized. The main advantage of SCWO over competing technologies such as incineration or wet oxidation is rapid (on the order of seconds), nearly complete destruction of hazardous waste to relatively innocuous compounds (e.g., CO_2, H_2O, NaCl, or N_2, etc.) in a closed system. For example, tests at Sandia National Laboratory have demonstrated that 99.99% destruction efficiency over a 15-second residence time can be obtained at 550°C and 3800 psi for military smokes and dyes (Rice et al., 1994). Currently, SCWO appears to be less likely to suffer from the NIMBY (Not In My Back Yard) syndrome than competing technologies. Many of the waste oxidation reactions in SCWO are exothermic, meaning that heat produced during oxidation can be used to reduce the overall energy requirements

4

and hence cost of the process. Furthermore, not only DoD hazardous wastes, but also DOE wastes and many municipal and industrial wastes appear suitable for destruction with SCWO, and it is estimated that SCWO will develop into a billion-dollar-a-year industry.

However, there are some technical problems which must be solved before SCWO can be used routinely in waste destruction. First, during oxidation of wastes containing chlorine, phosphorus or sulfur, dissolved acids and salts are generated which can lead to corrosion of the apparatus, unless a suitably resistant material can be found. Second, at constant pressure under supercritical conditions, the solubility of most salts is retrograde (i.e., decreases with increasing temperature). Precipitation of salts can interfere with reactor efficiency if not recognized and dealt with via appropriate reactor design and adjustment of operating conditions. Third, the presence of salts can cause a dramatic increase in the critical point of the aqueous phase. Because many of the desirable properties of SCWO depend on the presence of a one-phase, supercritical fluid, it is necessary to understand the effects of added components on the phase equilibria of water.

In SCWO, the reactor environment typically contains a fluid consisting of greater than 50% water, plus oxygen and carbon dioxide. In the case of DoD wastes, where S-, Cl-, F-, N-, and P-bearing compounds may be present, the fluid may also contain a wide range of acids, bases and salts. The expected operating conditions of most SCWO reactors is in the range 400°C to 700°C at about 250 bars. The major products of oxidation of most organic hazardous wastes are H_2O and CO_2. Chlorinated hydrocarbons will yield HCl, which may react with alkali (often added intentionally to neutralize the acid) to form alkali chloride salts. Sulfur is

oxidized to form sulfuric acid and phosphorus to phosphoric acid, which will form sulfate and phosphate salts upon reaction with alkali. Any F-bearing compounds will result in the presence of hydrofluoric acid. Nitrogen is converted to N_2 or N_2O, and the formation of NO_x, which occurs in conventional incineration, is avoided.

The chemical complexity of the SCWO reactor environment, coupled with the high temperatures and pressures required, presents a great challenge for material selection and reactor design. It has been found that extrapolation of materials performance to SCWO conditions based on previous experience in chemical process or steam generation equipment is unsatisfactory. Testing has suggested, for example, that stainless steels and high nickel alloys such as Hastelloy C-276, which are often satisfactory in other applications, exhibit unacceptable corrosion rates for waste streams containing salts, acids and bases (Barner et al., 1992; Garcia et al., 1995; Hazlebeck et al., 1995; Hong et al., 1995). Thus, these metals are probably unacceptable for use in SCWO reactors designed for DoD waste.

It should be mentioned that U.S. DOE hazardous wastes share some of the corrosive characteristics of DoD wastes. Both of these waste types are unique compared to the bulk of standard industrial and municipal wastes in the generation of corrosion problems. Although the volume of DoD and DOE wastes to be treated by SCWO is potentially very large, the volume of other less corrosive waste types is orders of magnitude larger. Thus, much research and development of SCWO in private industry has not been geared towards DoD needs, except when under DoD contract.

According to Modell (1995), there are essentially two mechanisms of corrosion in SCWO reactors. The first type occurs as a result of the

dissociation of HCl(aq) and other acids to H^+ and Cl^- upon cooling, and the consequent increase in fluid acidity. The second type is due to deposition of salts which occurs on heating. The former type of corrosion can be reduced by adding alkali to neutralize the acid, but at the expense of increasing the second type of corrosion. The second type of corrosion can be controlled by appropriate reactor design, i.e., elimination of dead spaces, maintenance of high fluid velocity, use of brushes, etc. Indeed, much progress has been made in innovative designs for the handling of salts in SCWO reactors (cf. Latanision & Shaw, 1993; Hazlebeck et al., 1995; Ahluwalia et al., 1995; McGuiness, 1995; La Roche et al., 1995; Fassbender et al., 1995). However, it is still necessary to construct SCWO reactors and associated equipment from materials which can withstand moderate degrees of corrosion, but which are at the same time, economically feasible.

The aim of this study was to examine the corrosion of various metals into aqueous fluids under typical conditions obtained in Supercritical Water Oxidation (SCWO) reactor systems. This study was designed to measure the corrosion rates of Pt, Au, Ti, Ta, Niobium, Zr and Hastelloy as a function of temperature, acidity, salinity and fluid oxygen content. The simplified experimental system used fluids which contained chlorine, rather than the mixture of halogens, S, and P which might be more typical of a DoD waste stream.

EXPERIMENTAL TECHNIQUES

Coupons of each metal were subjected to corrosion in convectively stirred static reaction vessels. Diagrams of the experimental setup for

7

the two different types of reaction vessel used are shown in Figures 1 and 2. Experiments were conducted at temperatures of 200 and 400°C, salinities of 0 – 0.2 m NaCl, acid concentrations of 0 - 0.02 m HCl, and dissolved oxygen concentrations of 0 - 1 mol % (produced by addition of hydrogen peroxide to the experimental starting solutions). Table 1 lists the combinations of experimental temperatures and fluid compositions tested. Run pressure was held constant during the experiment. Experimental fluids were critical at 400°C and subcritical at 200°C; convective mixing of the fluids was achieved by maintaining a temperature gradient of approximately 20°C between the top and bottom of the pressure vessel. The sample was a coupon of metal foil approximately 1 cm^2 in area.

The coupon weight was measured before and (if possible) after the experiment to determine weight loss during the run by dissolution into the fluid. In addition, it was possible to sample the experimental fluid directly from the pressure vessel during the experiment. During each experiment, the fluid was regularly sampled to determine how its composition changed with time. The fluid samples were analyzed by ion chromatography, to determine their chloride contents, and by inductively-coupled plasma atomic emission spectroscopy (ICP-AES), to determine metals in solution. In addition to the metal being studied, other metals in the pressure vessel and pressure system, such as titanium, gold, iron and nickel, were also analyzed in the fluid samples. If a solid precipitate was present in the fluid or a new phase had clearly grown on the surface of the metal coupon, the phase was identified by x-ray diffraction (XRD) analysis.

8

Experimental problems

Difficulties with the experiments resulted in considerable modifications to the experimental apparatus as the work progressed, as well as to the overall goals of the experiments. The initial experimental setup called for titanium or gold-lined steel pressure vessels, connected with 316 stainless steel tubing and fittings. These pressure vessels were of two sizes: one liter and 300 milliliters. The highly corrosive nature of the experimental fluids resulted in extremely rapid degradation of the steel pressure tubing, fittings, and valve seats. It also caused severe pitting of the titanium vessels and dissolution of the gold liners. In many cases, it was impossible to achieve a successful experiment at a particular set of conditions because the system components would corrode through and the experiment would fail in a matter of hours or days. We decreased the concentrations of NaCl, HCl, and O_2 in the experimental fluids in an attempt to lower their corrosivity while maintaining a useful set of experimental conditions, but this was not sufficient to prevent corrosion failure of the pressure system.

We attempted to replace as many system components as possible with more resistant materials, although there are few components available "off the shelf" for use in high-pressure, high-temperature, extremely corrosive conditions. Several generations of different tubing arrangements were constructed out of components including titanium capillary tubing, gold-plated steel ferrules, titanium tees, and even high-pressure PEEK tubing and fittings (used down-flow from a heat exchanger). None of these proved to be entirely satisfactory, being subject to leaks, clogging, cracking, and corrosion. Titanium components

9

were resistant to corrosion, but titanium fittings are subject to galling and titanium tubing is only available in narrow diameters which are subject to clogging by particles or corrosion products.

The problem of pressure vessel and liner corrosion also caused considerable difficulties, for pitting particularly attacked the gasket seal of the pressure vessels and tended to cause leakage and failure of the experiments. Some success was obtained by using Pyrex glass liners, obtainable only for the 300 mL pressure vessels. Although silica is somewhat soluble under the experimental conditions and the Pyrex liners slowly dissolved, this effect was slower and less extreme than the corrosion of the metal vessels and liners. In addition, the glass liners are inexpensive and expendable. Because the 300 mL vessels were limited in their working pressure – temperature range, however, only experiments at 200°C could be conducted in glass-lined vessels. The experiments at 400°C could only be run in the 1L vessels, and were subject to the constant problem of corrosion damage to the metal vessels and/or liners.

We attempted to circumvent the problem of corrosion of the pressure vessels by having several vessels coated with a permanently affixed layer of PFA Teflon. This lining was ineffective, for the thin Teflon membrane was permeable to water vapor during the high-temperature experiments. Water vapor diffused through the Teflon and formed bubbles which caused the coating to detach from the pressure vessel walls.

Initially all experiments in this study were designed to be run at a constant pressure of 4300 psi. Because of severe corrosion of the steel high-pressure tubing originally used in these experiments, we have had to switch to 1/16" titanium tubing which has lower pressure tolerances than

the steel. Thereafter, all successful subcritical experiments (those at 200°C) were run on the liquid-vapor curve (pressures of approximately 300 psi, depending on fluid composition). Supercritical experiments at 400°C were run at maximum pressures of 3000 psi.

The problem of pressure vessel corrosion also prevented completion of a significant portion of the proposed work. Our original intent was to complement the static experiments in this study with experiments done in a flow-through reactor, which would facilitate the measurement of dissolution rates of the metals under study. However, the immediate corrosion problems with the static vessels, which were composed of more resistant metals than the flow-through pressure vessel, made it necessary to re-evaluate this work. The flow-through vessel is composed of A-286 alloy. After the vessel was purchased, subsequent work in this laboratory in other vessels fabricated from this alloy demonstrated that it is extremely susceptible to stress corrosion cracking under chloride-rich conditions similar to those in the experiments in this study. We attempted to design a gold liner which would protect the vessel from contact with the experimental fluids and prevent cracking. The flow-through design of the reaction vessel, however, made it impossible to produce a liner which completely protected the vessel.

Results of modeling (Eh-pH diagrams)

The expected behaviors of the different metals under study may be predicted using pH- fO_2 diagrams (Brookins, 1988). The pH- fO_2 diagrams for several of the metals under study have been calculated using

11

thermodynamic data from Barner and Scheuerman (1978), Latimer (1952), and Wagman et al (1982).

Under the entire range of conditions examined in these experiments, the metals being studied are stable as oxides rather than as reduced metal phases. This is illustrated on the pH- fO_2 diagrams in figs. 3-6. Although chloride is present in abundance in the experiments, thermodynamic calculations show that metal chloride phases are never stable; our experimental results confirm this, as discussed below. At acidic conditions, the metals under study may be soluble in ionic form (figs. 3-6).

Many metals are stabilized under oxidizing conditions by the formation of a thin passive surface layer. Under some conditions, a metal oxide phase will form a thin film on the metal surface which prevents further oxidation of the metal. Although the ambient conditions may be in the stability range of the metal oxide rather than the reduced metal, the passive oxide coating will protect the metal beneath it. Under most of the experimental conditions, however, this behavior did not occur. Instead, the outer oxide coating which formed on the metal rapidly grew thick and flaked away, exposing fresh metal surfaces to the oxidizing fluid. Therefore the metal coupon was always exposed to the actual pH- fO_2 conditions and was rapidly consumed.

We did not test "pickling" processes, which are designed to develop a protective coating on metal surfaces before they are exposed to corrosive conditions. It is possible that such pre-treatment of some metals would somewhat improve their performance under the experimental conditions.

Experimental results for individual metals

Zirconium

Figure 7 shows dissolved concentrations of Zr plotted versus time for two experiments. This plot demonstrates the interesting and apparently self-contradictory behavior of Zr in the experimental fluids. In the experiment at #1 conditions (cf. Table 1), the highest concentrations of Zr are obtained early in the experimental run. Dissolved metal concentrations then fall off rapidly with time until they are below the detection limits of the ICP-AES. A possible explanation for this behavior is that the metals in solution are rapidly oxidized, and that the oxide phases have very low solubilities. However, at #3 conditions, the observed dissolved Zr contents are below the detection limit for most of the run, rising to 20 – 25 ppb shortly before the experiment failed. Figure 2 shows that ZrO_2 was expected to be be present in concentrations of at least 100 ppb under these conditions (Figure 2).

We were unable to obtain generally reliable solubility data for experiments on zirconium. In experiments on this metal, the sample coupon generally had completely corroded away by the end of the run, and the only solid phase remaining was the oxide baddleyite (ZrO_2), identified by x-ray diffraction (Figure 8) as well as mass balance of the run products. This suggests that, under the experimental conditions, the metal oxide layer on the surface of the metal coupon tends to thicken and flake off rather than protecting the metal beneath. The solubility of ZrO_2 is extremely low as mentioned above; most analyses for Zr in the experimental fluids were near or below the detection limits on the ICP-

AES. These results suggest that Zr is probably unsuitable for use in SCWO systems, for they were comparable across the range of conditions studied in these experiments.

Niobium

The observed behavior of niobium in the experiments was very similar to that of Zr. No Nb was detectable by ICP-AES in any of the experimental fluids. Niobium was not expected to be soluble under the experimental conditions (Figure 3).

Due to this solubility behavior, we were unable to obtain any reliable solubility data for experiments on niobium. As with zirconium, in experiments on this metal, the sample coupon would completely corrode away by the end of the run. The only solid phase remaining was the oxide Nb_2O_5, identified by x-ray diffraction (Figures 9 - 10) as well as mass balance of the run products. In an experiment at 400°C, 0.02 m NaCl, 0.02 m HCl, but containing no added oxygen, the oxide precipitates included not only Nb_2O_5 but also iron niobium oxide and possibly manganese niobium oxide (Figure 10). The iron and manganese in these solids apparently came from dissolution of the stainless steel tubing into the experimental fluid. Experiments in which the run was terminated almost immediately by corrosion failure of the pressure system showed that complete conversion of the Nb metal coupon to the oxide form occurred in less than 48 hours. As with Zr, the experimental results suggest that this metal is completely unsuitable for use in SCWO reactors.

Tantalum

Ta is extremely resistant to corrosion under the experimental conditions. This resistance appears to encourage corrosion of other metal components in the system in place of Ta. Experiments in progress were often terminated prematurely by clogged tubing or fittings as a result of this corrosion. The titanium alloy pressure vessels in which the experiments were conducted also suffered severe corrosion via the formation of deep pits in the vessel walls and head and at the gasket seal; oxides of titanium were deposited as a sludge on the vessel floor (Figure 11). Experiments in gold-lined vessels were not suitable for measuring the solubility of Ta, for they resulted instead in gold-plating of the Ta metal coupon. Experiments at 200°C were conducted in glass-lined vessels to avoid these problems as much as possible, but it was not possible to complete the sequence of experiments at 400°C due to extreme corrosion damage to the pressure vessels.

In none of the Ta dissolution experiments did the Ta foil lose measurable weight during the run. Dissolved Ta concentrations in these fluids were less than 500 ppb and these concentrations were only reached after run times of over 400 hours (Figure 12). The solubility of Ta, as with the other metals studied, should be controlled by an oxide phase rather than by the reduced metal under these conditions (Figure 4). Formation of tantalum oxides was not observed in most of the experiments, at least at the level of detectability by XRD. An unsuccessful experiment at #8 conditions (Table 1) did result in formation of a brown, powdery oxide coating on the Ta foil; this coating was identified by XRD as being a mixture of $Ta_{0.8}O_2$ and Ta_2O_5 (Figure 13).

This coating did not exhibit the flaking behavior observed in other metals such as Zr and Nb, and may have served as a protective coating for the metal underneath, for the coupon gained weight during the experiment as would be expected from the formation of the oxide.

Titanium

Titanium reached higher dissolved concentrations in the experimental fluids than did Zr, Nb, or Ta. Figure 14 shows typical behavior for dissolved Ti with time; concentrations of the metal tended to peak early in the experiment and then tail off. Possibly this reflects initial oversaturation of the fluid with Ti, followed by precipitation of TiO_2.

Like Nb and Zr, titanium also forms an oxide phase with an extremely low solubility during the experiments (e.g., Figure 5). This oxide has been identified by its x-ray diffraction spectrum to be the mineral rutile (Figures 11 and 15). Under some experimental conditions this oxide displays a similar behavior to the Zr and Nb oxides, in that it forms a coating on the Ti surface which then flakes off to expose unreacted metal to the fluid. Under most experimental conditions, however, the Ti coupon is apparently unaffected by reaction with the experimental fluids and is not soluble in the fluid. It is likely that, in these experiments, a passive Ti-oxide film is coating the surface of the metal and preventing further reaction with the fluid.

It is possible that under some conditions the oxide being formed is some metastable phase such as the mineral anatase, rather than the more stable polymorph rutile. X-ray diffraction of the solids formed in one experiment at #1 conditions (Figure 15) appears to show a small

amount of anatase mixed with the more abundant solid rutile. Anatase has a somewhat higher solubility than rutile under the experimental conditions (Brookins, 1988). If anatase forms first and later converts to rutile, this could explain the bell-shaped form of the concentration curve in Figure 14.

During experiments in Ti vessels on other metals, the Ti vessels often displayed a striking lack of corrosion resistance. Experiments on Ta in particular showed extreme pitting corrosion of the pressure vessel walls, the vessel head, and the gasket seal. Often this pitting appeared to have been initiated at the contact between gasket and vessel, but this was not always the case. This corrosion of the vessel may have been exacerbated by galvanic effects. These observations suggest that, although titanium is both inexpensive and resistant to corrosion, it should not be used in a SCWO system together with more noble metals which could substantially shorten its lifetime.

316 stainless steel

While these experiments were not initially designed to examine the corrosion of steel, as noted above, there was considerable corrosion of distal parts of the pressure system by the experimental fluids. Many of these pressure components were constructed of 316 stainless steel (nominal composition Fe / Cr 18 / Ni 10 / Mo 3 / Mn). Because dissolution of steel components was adding metals (sometimes in high concentrations) to the experimental fluids, it was necessary to monitor the concentrations of these elements in the fluids. Under some circumstances, it may be that corrosion of the steel was accelerated by

formation of a galvanic cell with the more resistant metals under study, and that this may have depressed dissolution of the metal samples.

The concentrations of elements corroded from the steel exhibited a number of interesting behaviors, for there was clear preferential dissolution of certain elements into the experimental fluids. Figure 16 shows the dissolved content of Fe, Cr, Ni, Mo and Mn in experimental fluids, compared with the nominal content of commercial 316 stainless steel. It appears from this figure that Ni and Mn are preferentially extracted from the metal into the fluid. Chromium appears to resist dissolution under most experimental conditions, whereas iron is sometimes resistant but is sometimes preferentially removed from the metal.

Figures 17 and 18 show that Cr and Mo exhibit the same behavior noted earlier in several other metals: their dissolved concentrations peak early in the experiment and then tail off to very low values. Once again, this may reflect early oversaturation of the fluid with these metals followed by precipitation of solids.

Hastelloy C

Dissolution data on Hastelloy C foil (composition according to supplier: Ni57 / Mo17 / Cr16 / Fe / W / Mn) have been collected at 200°C only; these are the odd-numbered sets of conditions in Table 1. It proved impossible to complete an experiment at the 400°C conditions; these experiments consistently corroded through some portion of the pressure system and failed. Data from a long-running experiment on Hastelloy are shown in Figure 19. This experiment was conducted at the

7 conditions: 0.02 m HCl, 0.2 m NaCl, and 0.1 mol % O_2. Time series of samples from this experiment indicate that equilibrium between coupon and fluid is reached after a period of ~400 hours (Figure 19). The dissolution behavior of Hastelloy under these conditions is similar to that observed in this study for 316 stainless steel. Results for both 316 SS and Hastelloy show preferential dissolution of certain metals into the experimental fluid which bear little relation to the concentration of those metals in the alloy. Metals which have been preferentially leached are Fe, Ni, and to some extent Mn. Other metals including Cr, Mo and W appear to preferentially remain in the solid phase under these conditions. The less soluble metals may form a passive film on the surface of the metal coupon, but if so this film is not voluminous enough to be detected as a separate oxide phase by X-ray diffraction (XRD) as shown in Figures 20 - 21. Figure 20 shows the XRD spectrum of an unreacted Hastelloy metal coupon. Figure 21 shows a scan of the coupon from the experiment discussed above after the completion of the run at #7 conditions. No oxide phases are observable in the XRD scan, but Figure 21 does show that gold metal from the gold pressure vessel liner was plated on the surface of the Hastelloy coupon.

The Hastelloy coupon in this experiment lost a total of 18 mg through dissolution after approximately 700 hours of reaction time with 300 ml of fluid. The actual weight loss through dissolution of Hastelloy may have been greater, as the thin film of gold plated onto the foil (Figure 20) may have increased its weight somewhat. If the true weight loss were 18 mg then this would imply maximum dissolved metal contents of 60 ppm, several times lower than the actual peak measured concentrations of dissolved metals. There are two possible explanations

for this which are not mutually exclusive. The first is that gold deposition on the Hastelloy foil significantly changed its weight. To completely explain the discrepancy this would require deposition of ~60 mg of gold on the foil, which seems highly unlikely. The second possibility is that some of the dissolved Ni and Fe present in the sampled fluid actually came from dissolution on the surfaces of steel components (valves and fittings) in the pressure system. As dissolution of steel components has been an ongoing problem in this study, it is likely that this process occurred.

At the end of this experiment a considerable amount of powdery, red, suspended sediment was recovered with the run fluid from the pressure vessel. An XRD scan of this sediment shows it to be composed almost entirely of hematite (Fe_2O_3) with small amounts of gold (Figure 22). The gold detected comes from the pressure vessel liner but must have been recrystallized in order to appear in the sediments; possibly it precipitated on the Hastelloy foil or the Ti pressure vessel head but later flaked off.

The transport and re-precipitation of gold metal in this experiment suggests that a galvanic cell was set up between gold and metals in the Hastelloy foil. Dissolved gold contents were below detection limits in the fluid, implying that the extent of actual gold transport through the fluid was limited by low solubility. However, this suggests that the measured concentrations of other metals in the fluid may have been affected by the galvanic action.

Figures 23 and 24 show data from a Hastelloy dissolution experiment run at #1 conditions: 0.002 m HCl, 0.02 m NaCl, and 0.1 mol % O_2. The dissolved metal concentrations in this experiment show rather

different behavior from that shown in Figure 19 for #7 conditions. Overall dissolved metal contents in the fluid are much lower than in the previously discussed experiment, as might be expected for these less extreme conditions. Yet despite the lower overall dissolved concentrations, a larger number of different metals are present in measurable concentrations in these fluids, including metals such as Au, Cr and Mo which were insoluble at the #7 conditions. As with the experiment at #7 conditions, the foil in this experiment was plated with gold by the end of the run (Figure 25)

Figure 26 shows data from an experiment run at #3 conditions: 0.02 m HCl, 0.02 m NaCl, and 1 mol % O_2. This experiment also exhibits interesting trends in dissolved metal concentrations with time. Total dissolved metal concentrations are comparable to those at #1 conditions, but high Au concentrations (up to 12 ppm) were present in fluid samples. The dissolved concentration of Au is apparently paralleled by the concentrations of Cr and Mn. This result suggests that the solubility of metals such as Cr and Au increase when both the HCl concentration and the oxygen content are high. The high concentrations of Au in this fluid suggest that large amounts of Au are being mobilized from the pressure vessel liner and may be plating out onto other metal components, such as the Hastelloy foil as observed in other experiments.

Gold

Gold metal has not been observed to form a non-metallic solid reaction product under any conditions tested. Gold is relatively soluble in the fluid under Cl-rich conditions and this solubility is further enhanced by

21

addition of oxygen to the fluid; however, data on Au concentrations in our experiments may not be reliable due to the effects of other elements on dissolved Au concentration, as discussed above in the sections on Ta, Ti, and Hastelloy. For example, Figure 27 shows Au concentrations vs. time for experiments at three different sets of conditions. These concentrations never reach a plateau, even after other dissolved metal concentrations in the solution have done so; rather, they fluctuate continually. This observation implies that these concentrations do not reflect true solubility, but instead result from galvanic processes.

In many dissolution experiments intended to examine other metals but run in gold-lined pressure vessels, Au was dissolved from the vessel liner and reprecipitated on the metal coupon, the Ti pressure vessel head, the Ti wire sample holder, and on various other metal system components. Crystals of this gold were generally also identifiable in the sediment at the bottom of the pressure vessel at the end of the experiment. This tendency of gold to act as an anode, enter the solution in high concentration, and plate onto other metals certainly suggests that it would be a highly unsuitable metal for use in SCWO reactors unless it could be isolated from contact with any other resistant metals.

Conclusions

We were unfortunately unable to complete much of the intended work of this study due to technical problems with the equipment, particularly corrosion and failure of the pressure vessels, tubing, valves, and other components of the pressure system. It is somewhat ironic that a study of corrosion should be so hampered by corrosion. However, the

experimental results do point qualitatively towards some promising directions for research into possible metal liners for SCWO reactor systems.

Our study found that Zr and Nb are both likely to be unsuitable for use in SCWO systems, for they rapidly converted under the experimental conditions to oxide forms. Rather than forming passive, protective coatings, these oxides ablated off the sample coupons and formed a sediment in the pressure vessel. Thus, if these metals were used in a SCWO reactor, they would not only be likely to fail extremely rapidly but they would also foul the system in doing so.

Hastelloy has previously been found to be unsuitable for use in SCWO reactors (Boukis et al, 1995; Hong et al, 1995) due to extremely rapid corrosion. The Hastelloy samples in this study did exhibit a certain amount of dissolution, but the extent of this dissolution was largely inhibited by galvanic effects and the Hastelloy coupons often acted as cathodes on which other metals were plated. However, prevous work certainly suggests that Hastelloy is an unsuitable metal for use in SCWO systems and therefore we can not recommend its use.

The behavior of gold in our experiments was dominated by galvanic effects which caused it to dissolve and reprecipitate on other metal surfaces. This behavior caused gold surfaces to erode rapidly, for substantial amounts of the metal were being transported through the experimental fluid although dissolved concentrations were usually on the order of several ppm or less. This behavior suggests that gold will not be acceptable for use in any SCWO system in which other metals are also present. The experimental design made it impossible to evaluate the behavior of gold in the complete absence of other metal surfaces.

Previous studies have suggested that titanium is a promising metal for use in SCWO systems. The results of this study for titanium were mixed. Titanium coupons were largely unaffected by the experimental fluids and any weight loss from them was undetectable. But the titanium pressure vessels and, to a smaller extent, titanium pressure tubing, were subject to corrosion which often caused failure of the experiments. Pitting corrosion of the pressure vessels was a constant problem and was often severe, forming pits of over 1 cm deep and requiring re-machining of the vessels. This pitting often appeared to initiate at pre-existing irregularities such as corners, edges, or the crack between pressure vessel and gasket. It is possible that smoother surfaces would have minimized pitting by providing fewer nucleation sites. However, reducing the chloride content of the fluids would likely also improve the resistance of titanium to pitting, and so it may be an excellent metal for use in less corrosive solutions.

Tantalum was by far the most resistant metal to dissolution or corrosion in this study. Tantalum coupons survived many weeks of immersion in the experimental fluids and generally emerged with no apparent weight loss. The chemical resistance of tantalum suggests that it is an excellent candidate for use in SCWO systems; its main drawback might be the difficulty of working it, rather than any problems with corrosion.

List of References Cited

Ahluwalia, K.S., Young, M.F., Haroldsen, B.L., Mills, B.E., Stoddard, M.C. and Robinson, C.D. (1995) Testing and application of a transpiring wall platelet reactor for supercritical water oxidation of hazardous waste. First International Workshop on Supercritical Water Oxidation. Jacksonville, Florida. February 6-9, 1995.

Barner H.E. and Scheuerman R.V. (1978) Handbook of thermochemical data for compounds and aqueous species. Wiley & Sons, New York, 156 pgs.

Barner, H.E., Huang, C.Y., Johnson, T., Jacobs, G., Martch, M.A., and Killilea, W.R. (1992) Supercritical water oxidation: An emerging technology. Jour. Hazardous Mater., 31: 1-17.

Boukis, N., Lanvatter, R., Habicht, W., Franz, G., Leistikow, S., Kraft, R., and Jacobi, O. (1995) First experimental supercritical water oxidation corrosion results of Ni-based alloys fabricated as pressure tubes and exposed to oxygen containing diluted hydrochloric acid at T≤450°C, P=24 MPa. First International Workshop on Supercritical Water Oxidation. Jacksonville, Florida. February 6-9, 1995.

Brookins D.G. (1988) Eh-pH Diagrams for Geochemistry. Springer-Verlag, New York, 176 pgs.

Fassbender, A.G., Robertus, R.J. and Deverman, G.S. (1995) The dual shell pressure balanced vessel: A reactor for corrosive applications. First International Workshop on Supercritical Water Oxidation. Jacksonville, Florida. February 6-9, 1995.

Garcia, K.M. and Mizia, R. (1995) Corrosion investigation of multilayered ceramics and experimental nickel alloys in SCWO process environments. First International Workshop on Supercritical Water Oxidation. Jacksonville, Florida. February 6-9, 1995.

Hazlebeck, D.A., Downey, K.W., Elliott, J.P. and Spritzer, M.H. (1995) Design of corrosion resistant HTO systems for DoD hazardous wastes. First International Workshop on Supercritical Water Oxidation. Jacksonville, Florida. February 6-9, 1995.

Hong, G.T., Ordway, D.W. and Zilberstein, V.A. (1995) Materials testing in supercritical water oxidation systems. First International Workshop on Supercritical Water Oxidation. Jacksonville, Florida. February 6-9, 1995.

La Roche, H.L., Weber, M. and Trepp, Ch. (1995) Rationale for the filmcooled coaxial hydrothermal burner (FCHB) for supercritical water oxidation (SCWO). First International Workshop on Supercritical Water Oxidation. Jacksonville, Florida. February 6-9, 1995.

Latanision, R.M. and Shaw, R.W. (1993) Corrosion in supercritical water oxidation systems. Workshop Summary, MIT. MIT-EL 93-006.

Latimer W.M. (1952) Oxidation Potentials. Prentice Hall, Princeton, 392 pgs.

Marsh, J. (1995) Federal interagency perspectives on the potential applications of SCWO. First International Workshop on Supercritical Water Oxidation. Jacksonville, Florida. February 6-9, 1995.

McGuinness, T.G. (1995) Developments in transpiring-wall SCWO reactor technology. First International Workshop on Supercritical Water Oxidation. Jacksonville, Florida. February 6-9, 1995.

Modell, M. (1995) Industrial applications of SCWO: Dispelling the myths. First International Workshop on Supercritical Water Oxidation. Jacksonville, Florida. February 6-9, 1995.

Rice, S.F. et al. (1994) Supercritical water oxidation of colored smoke, dye, and pyrotechnic compositions. SAND94-8209.

Shaw, R.W., Brill, T.B., Clifford, A.A., Eckert, C.A. and Franck, E.U. (1991) Supercritical water: A medium for chemistry. Chemical & Engineering News, Dec. 23, 1991, 26-38.

Tester, R.W., Holgate, H.R., Armellini, F.J., Webley, P.A., Killilea, W.R., Hong, G.T. and Barner, H.E. (1993) in D.W. Teddear and F.G. Pohland, editors, Emerging Technologies in Hazardous Waste Management III, ACS Symp. Ser. 518.

Wagman D.D., Evans W.H., Parker V.B., Schumm R.H., Halow I., Bailey S.M., Churney K.L. and Buttall R.L. (1982) The NBS tables of chemical thermodynamic properties. Selected values for inorganic and C2 and C2 organic substances in SI units. J Phys Chem Ref Data 11, suppl. 2.

PERSONNEL SUPPORTED UNDER THIS PROJECT

Scott A. Wood, Ph.D., Professor of Geochemistry

Leslie L. Baker, Ph.D., Postdoctoral Fellow

Yongliang Xiong, Ph.D. Candidate
    (Ph.D. Geology and Geological Engineering, 1999)

Julie Pickrell, M.S. Candidate
    (M.S. Geology and Geological Engineering, 1997)

Subramani Thiagarajan, M.S. Candidate

Deborah Agenbroad, B.S. Candidate
    (B.S. Geology and Geological Engineering, 1999)

Tables

Table 1: Experimental run conditions.

#	T (°C)	HCl (*m*)	NaCl (*m*)	mol % O$_2$
1	200	0.002	0.02	0.1
2	400	0.002	0.02	1
3	200	0.02	0.02	1
4	400	0.02	0.02	0.1
5	200	0.002	0.2	1
6	400	0.002	0.2	0.1
7	200	0.02	0.2	0.1
8	400	0.02	0.2	1

Figure captions

Figure 1

Diagram of experimental setup; 300 ml bolted-closure pressure vessel. The vessel cap bolts into the flange around the top of the vessel. This compresses the gasket ring between the cap and the vessel body and so forms the seal. Gold or Pyrex liners sit inside the body of the vessel. The sample metal coupon is suspended from a pyramidal holder constructed of gold or titanium wire. Two ports extend through the cap and allow external tubing to be attached to the vessel for sampling fluids in mid-experiment.

Figure 2

Diagram of experimental setup; 1L bolted-closure pressure vessel. The head is set on top of the vessel and the cap screws on over the head. The vessel is sealed by bolts in the cap which press on the head, compressing the gasket ring between the head and the vessel. Liners and the sample holder are as in Fig 1. The two sampling ports in this type of vessel extend vertically through the vessel head.

Figure 3

Oxygen fugacity versus pH diagram for Zr at 200°C and 1 bar. Calculated for $[Zr^{4+}] = 10^{-6}$.

Figure 4

Oxygen fugacity versus pH diagram for Nb at 200°C and 1 bar.

Figure 5

Oxygen fugacity versus pH diagram for Ta at 200°C and 1 bar. Calculated for $[TaO_2^+]=10^{-6}$.

Figure 6

Oxygen fugacity versus pH diagram for Ti at 200°C and 1 bar. Calculated for $[TiO^{2+}] = 10^{-6}$.

Figure 7

Concentrations of Zr in samples of the experimental fluids are plotted against run time. Different plot symbols indicate two different experimental runs at 200°C, 0.002 m HCl, 0.02 m NaCl, 0.1 mol % O_2 and 200°C, 0.02 m HCl, 0.02 m NaCl, 1 mol % O_2.

Figure 8

X-ray diffraction scan of solid precipitate formed during Zr corrosion experiment at 400°C, 0.02 m HCl, 0.02 m NaCl, 0.1 mol % dissolved O_2. X-ray diffraction pattern matches the indexed pattern for ZrO_2 (baddleyite).

Figure 9

X-ray diffraction scan of solid precipitate formed during Nb corrosion experiment at 200°C, 0.002 m HCl, 0.02 m NaCl, 0.1 mol % dissolved O_2. X-ray diffraction pattern matches the indexed pattern for crystalline Nb_2O_5. Unmatched peaks may be slightly different forms of Nb_2O_5.

Figure 10

X-ray diffraction scan of precipitate formed during Nb corrosion

experiment at 400°C, 0.02 m NaCl, 0.02 m HCl, but containing no

added oxygen. X-ray diffraction pattern matches the indexed pattern

for Nb_2O_5 but additional peaks also appear to indicate the presence of

iron niobium oxide and possibly manganese niobium oxide.

Figure 11

X-ray diffraction scan of solid precipitate formed during Ta corrosion

experiment at 200°C, 0.002 m HCl, 0.02 m NaCl, 0.1 mol % dissolved

O_2. This precipitate is apparently composed entirely of TiO_2 which

formed from corrosion of the titanium pressure vessel. The pressure

vessel was severely damaged in this experiment.

Figure 12

Plot of dissolved Ta concentration vs time in experiment at 200°C, 0.02

m HCl, 0.02 m NaCl, 1 mol % dissolved O_2. Ta reaches dissolved

concentrations of less than 50 ppb.

Figure 13

X-ray diffraction scan of Ta foil from experiment run at 400°C, 0.02 m

HCl, 0.2 m NaCl, 1 mol % dissolved O_2. The foil is partially covered

with a brown, powdery coating, identified here as being a mixture of

tantalum oxides.

Figure 14

Plot of dissolved Ti concentration vs time in experiment at 200°C, 0.002 m HCl, 0.02 m NaCl, 0.1 mol % dissolved O_2. Total concentrations above 1.5 ppm are reached early in the experiment, but then drop off to values of ~100 ppb.

Figure 15

X-ray diffraction scan of sold precipitate formed during Ti corrosion experiment at 200°C, 0.002 m HCl, 0.02 m NaCl, 0.1 mol % dissolved O_2. Most of the solid present is rutile, but some is anatase, a more soluble polymorph of TiO_2. Some crystalline gold is also present; it probably recrystallized from the pressure vessel liner during the experiment.

Figure 16

Figure comparing dissolved contents of Fe, Cr, Ni, Mo, and Mn in experimental fluids with starting composition of 316 stainless steel. This figure shows that some metals (Ni, Mn) are preferentially dissolved out of steel by the experimental fluids whereas others (Cr, Mo) are left behind.

Figure 17

Concentration of Cr plotted vs time in experimental fluids at several different sets of conditions. The concentration of Cr rises to its highest level early in the experiment, then drops rapidly and tails off with time.

Figure 18

Concentration of Mo plotted vs time in experimental fluids at several different sets of conditions. The concentration of Mo behaves like that of Cr, peaking early and then tailing off.

Figure 19

Plot of dissolved metal concentrations vs. time in Hastelloy C dissolution experiment at 200°C, 0.002 m HCl, 0.2 m NaCl, 1 mol % dissolved O_2. Absolute concentrations of these metals vary, but reach a plateau after ~400 hours.

Figure 20

XRD scan of unreacted Hastelloy foil coupon. The scan pattern is similar to that of 304 stainless steel.

Figure 21

XRD scan of Hastelloy foil from experiment run at 200°C, 0.02 m HCl, 0.2 m NaCl, 0.1 mol % dissolved O_2. Gold metal dissolved from the pressure vessel liner has been deposited on the foil coupon. No oxide phases are present in this scan.

Figure 22

Solid precipitate from same experiment as foil in Figure 21. Hematite and gold have precipitated from the experimental fluid. The gold precipitate formed from gold dissolved from the pressure vessel liner. Iron in the hematite is most likely at least partly dissolved from the

Hastelloy coupon, although some iron may come from the steel pressure system components as well.

Figure 23

Plot of dissolved metal concentrations vs time in a Hastelloy C dissolution experiment at 200°C, 0.002 m HCl, 0.02 m NaCl, 0.1 mol % dissolved O_2. The dissolved concentrations of Fe, Mn, and Mo are considerably lower than those shown in Figure 19 and plateau after approximately 300 hours run time.

Figure 24

Plot of dissolved metal concentrations in the same experiment as Figure 23. Dissolved concentrations of Ni are lower than those shown in Figure 19, but dissolved Cr concentrations are considerably higher than those in Figure 19. These experimental conditions apparently foster preferential dissolution of Cr from the metal coupon.

Figure 25

XRD scan of Hastelloy foil from experiment run at 200°C, 0.002 m HCl, 0.02 m NaCl, 0.1 mol % dissolved O_2. Gold metal dissolved from the pressure vessel liner has been deposited on the foil coupon. No oxide phases are present in this scan.

Figure 26

Plot of dissolved metal concentrations vs. time in a Hastelloy C dissolution experiment at 200°C, 0.02 m HCl, 0.02 m NaCl, 1 mol % dissolved O_2. Dissolved concentrations of most of these elements are higher than in

the experiment shown in Figures 23-24, but lower than the values in Figure 19.

Figure 27

Plot of dissolved gold concentrations in experiments at #1, 3, and 5 conditions (Table 1). Gold concentrations reach values above 10 ppm but fluctuate rather than reaching a stable plateau. This suggests that these concentrations do not reflect actual gold solubility under these conditions.

Figure 1

Figure 2

bolts for cap

pressure
vessel cap

pressure
vessel head

gasket

experimental
fluid

pressure

sample holder and
metal coupon
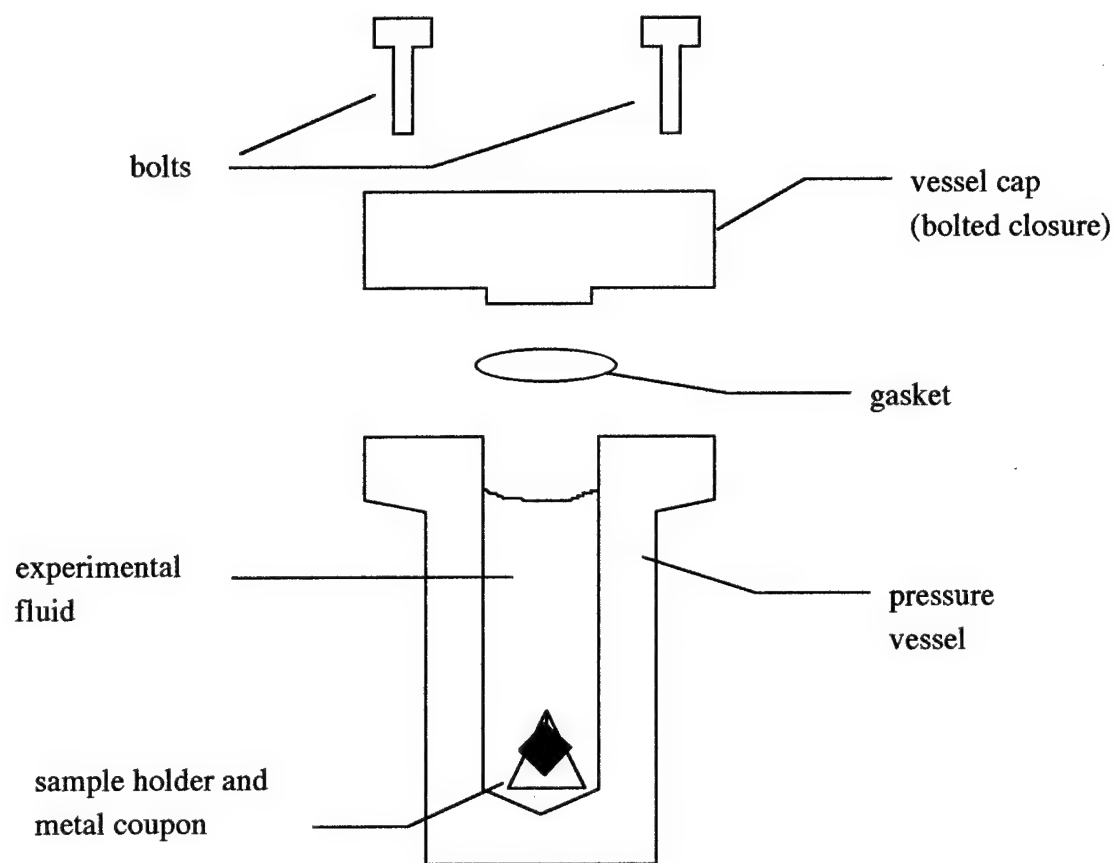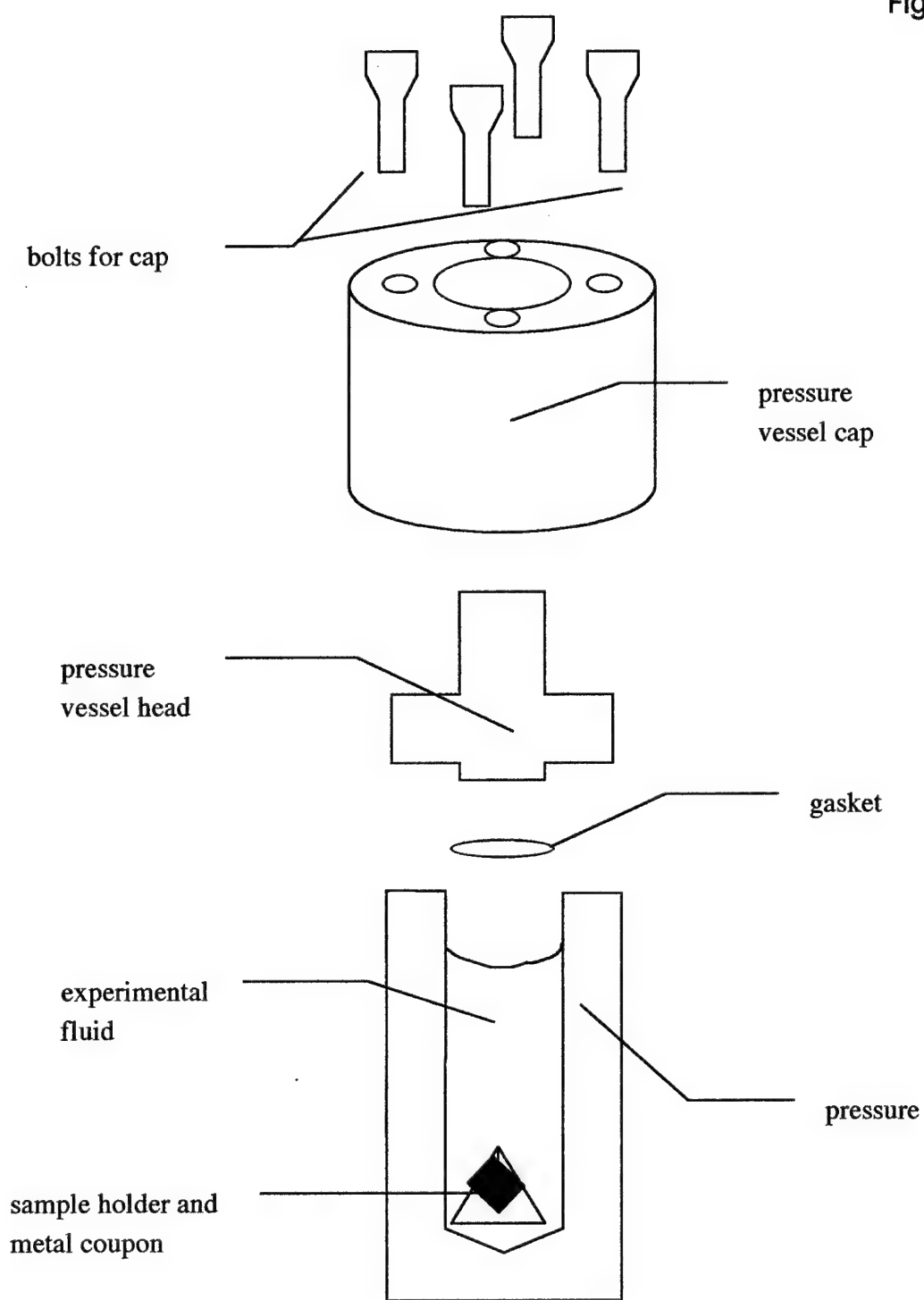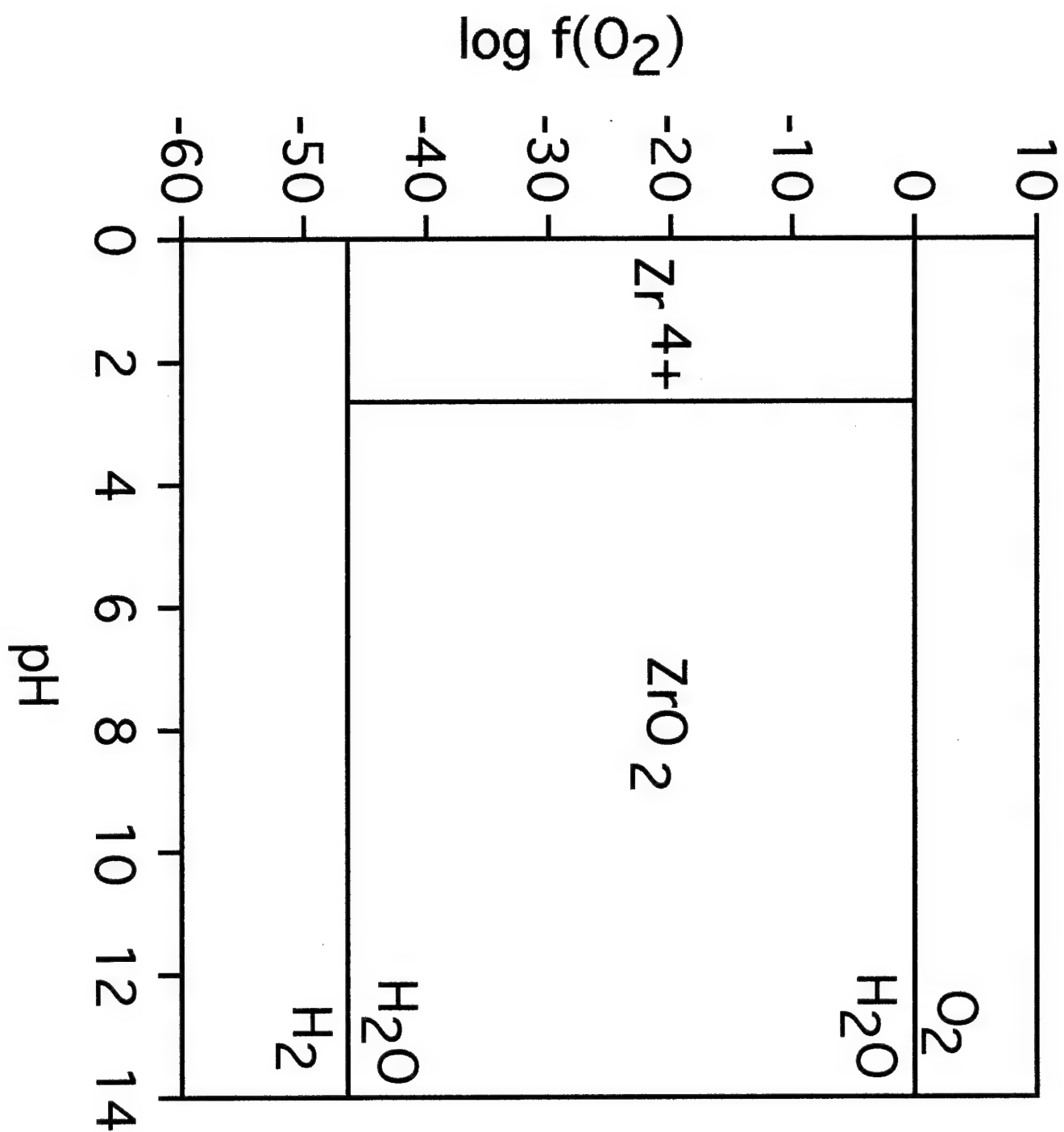
Figure 3
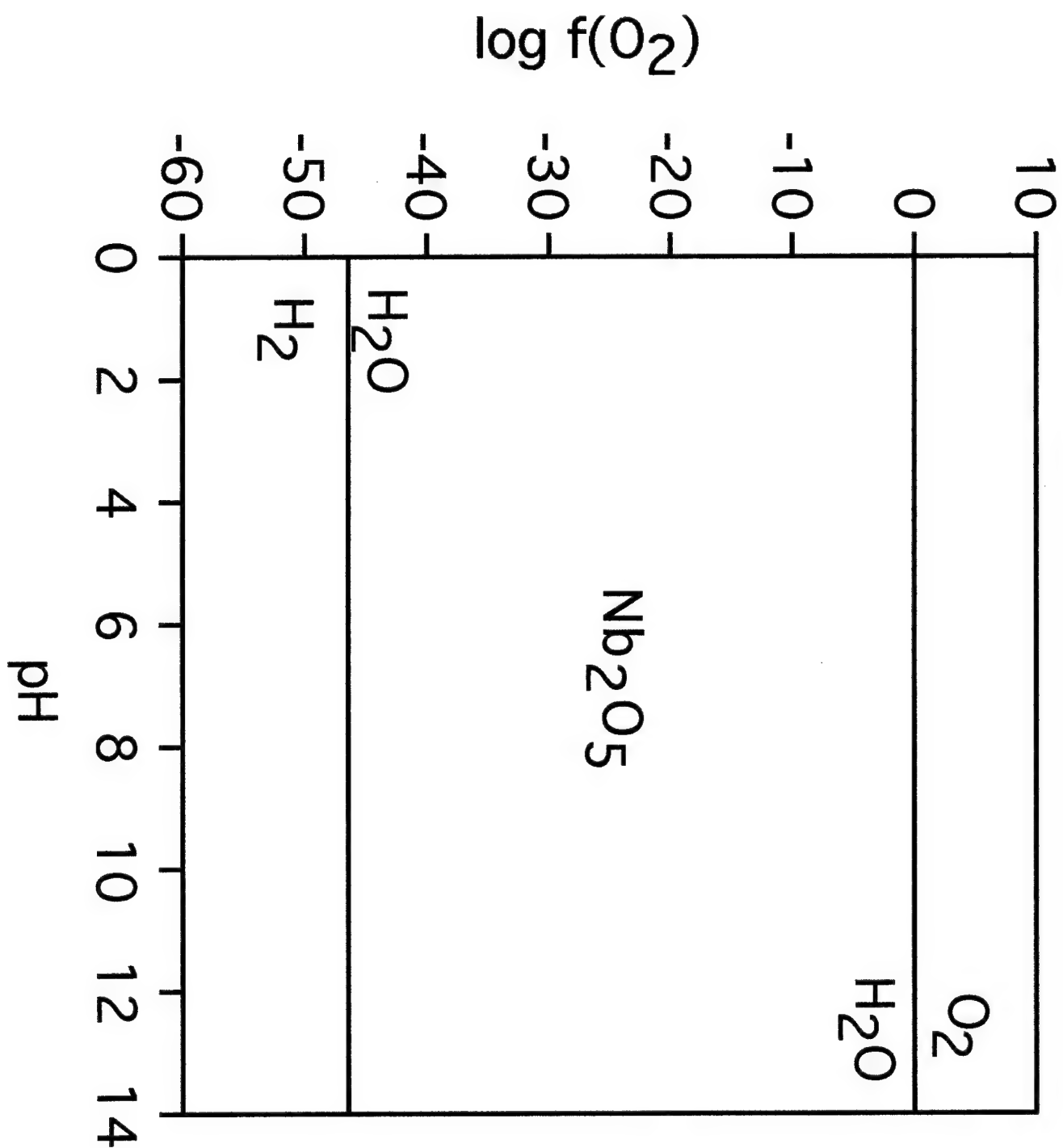
Figure 4

Figure 5
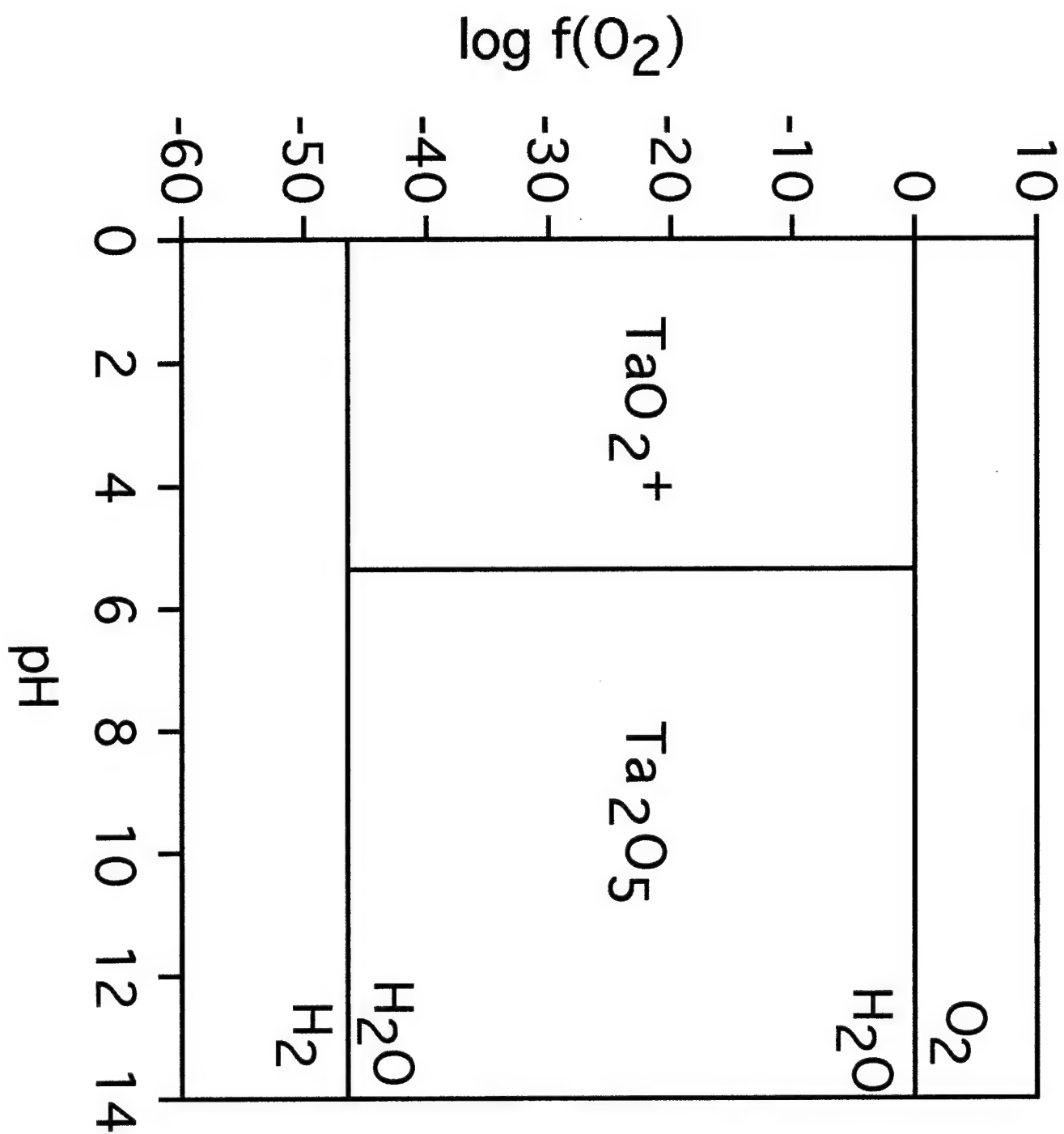
Figure 5
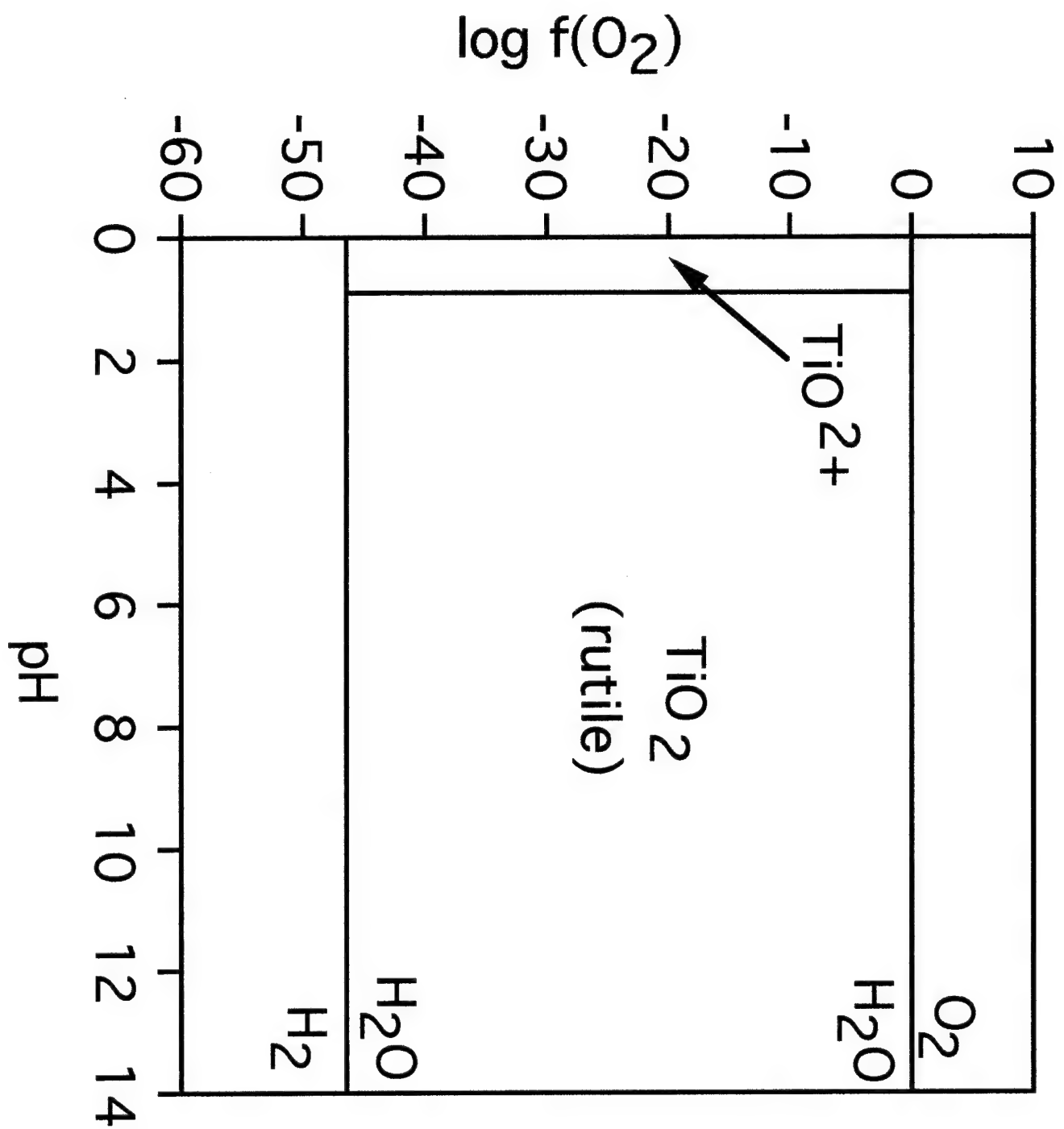
Figure 6
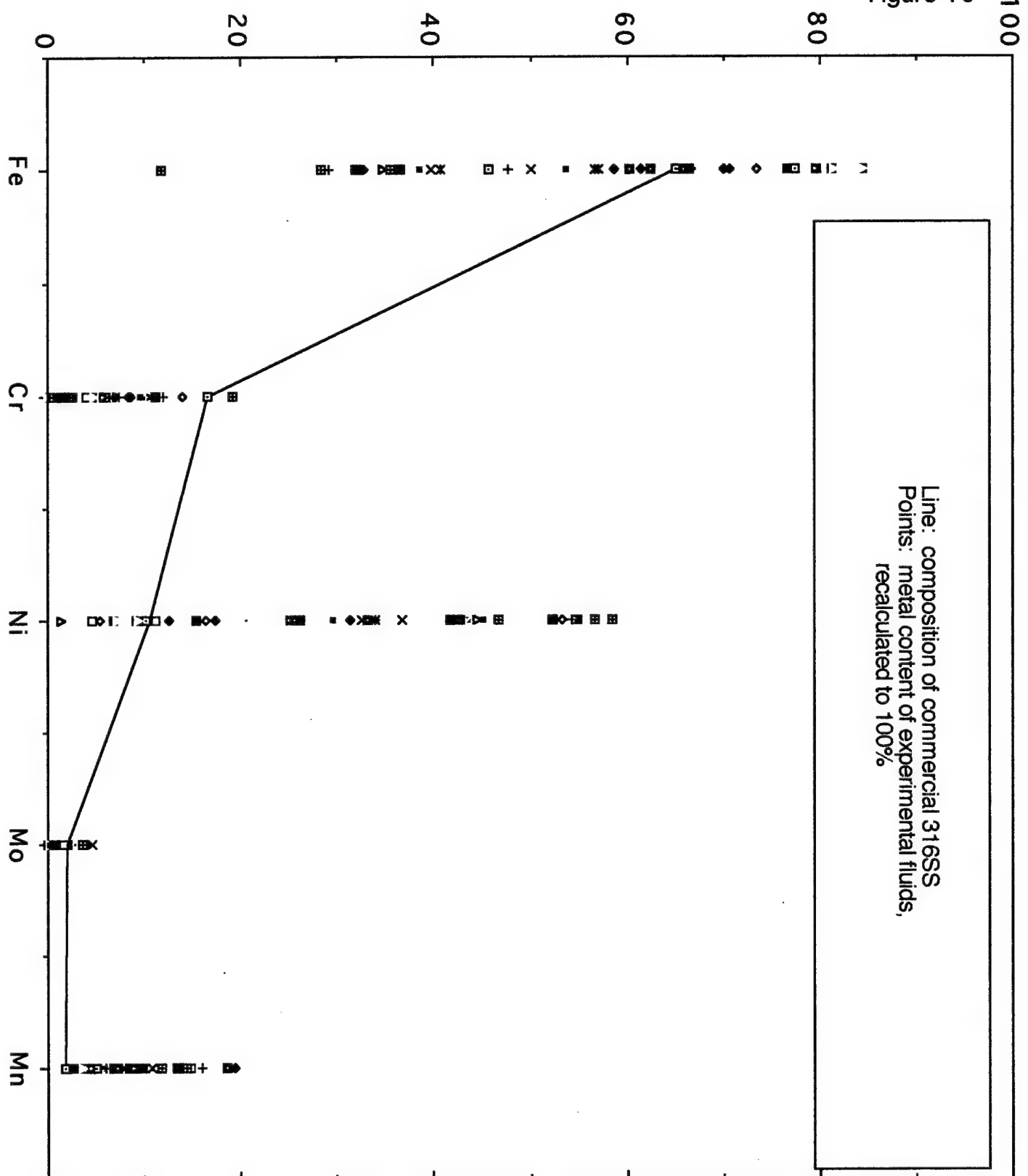
Figure 7
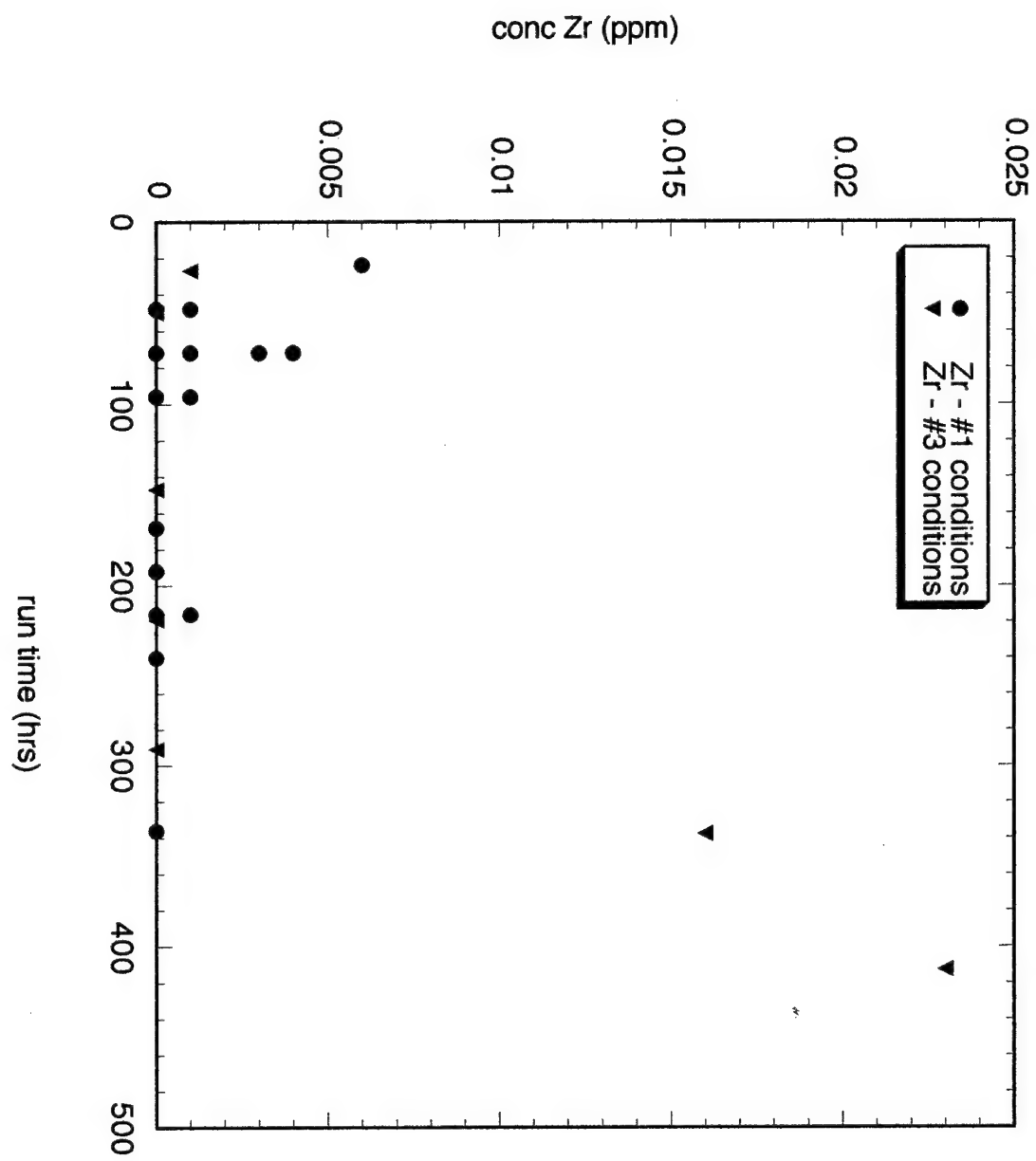
Figure 7
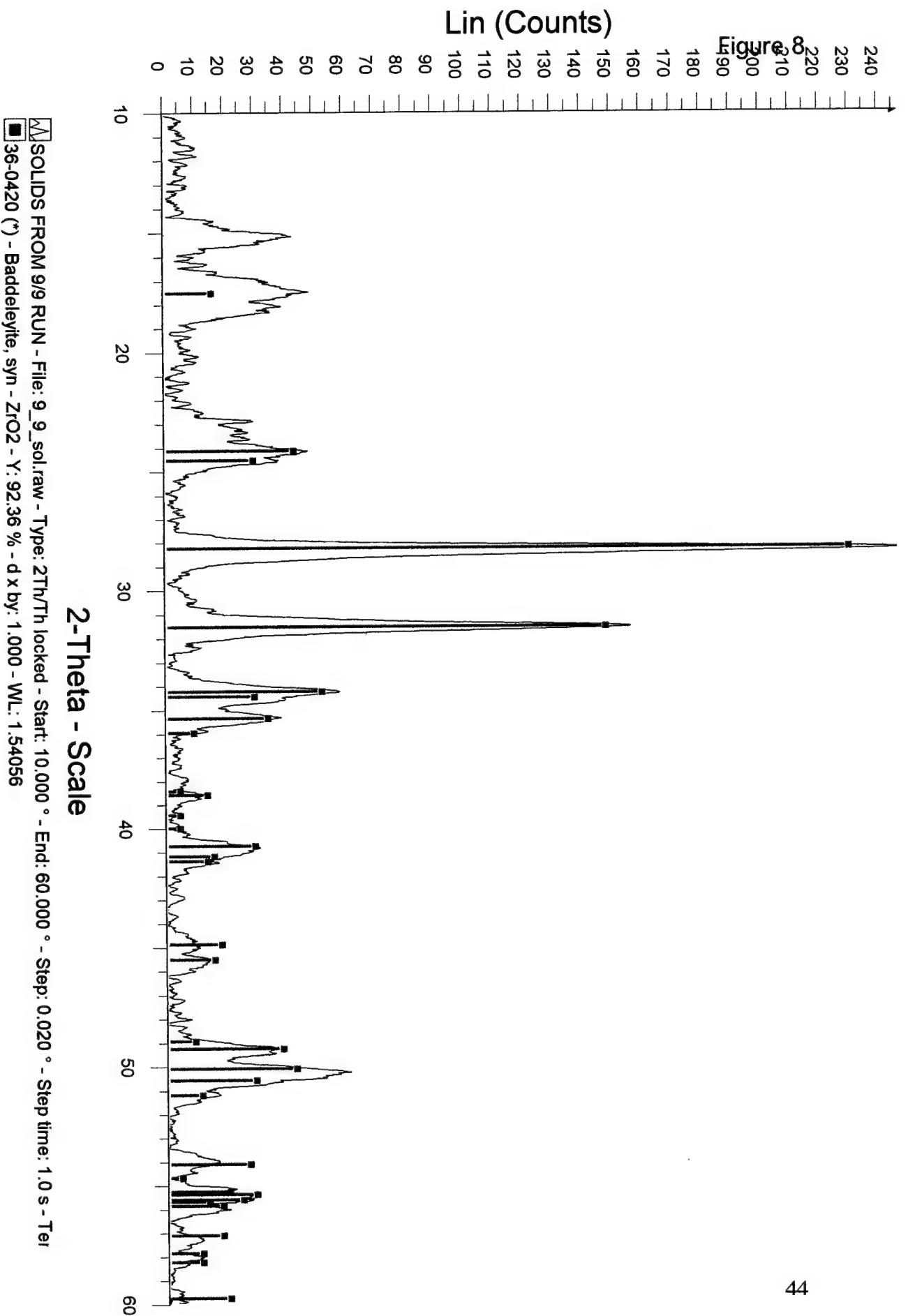
Figure 8

Figure 9

2-Theta - Scale

Lin (Counts)

solids frmo 10/23 expt (Nb) - File: 10-23-sol.RAW - Type: 2Th/Th locked - Start: 10.000 ° - End: 40.000 ° - Step: 0.020 ° - Step time: 1.0 s
■ 30-0873 (C) - Niobium Oxide - Nb2O5 - Y: 96.39 % - d x by: 1.000 - WL: 1.54056
● 29-0733 (*) - Ilmenite, syn - FeTiO3 - Y: 25.00 % - d x by: 1.000 - WL: 1.54056
▲ 41-1432 (*) - Pseudobrookite, syn - Fe2TiO5 - Y: 50.00 % - d x by: 1.000 - WL: 1.54056

45

Figure 10

Figure 11

2-Theta - Scale

Lin (Counts)

solids from 9/3 Ta expt - File: 9-3-sol.RAW - Type: 2Th/Th locked - Start: 10.000 ° - End: 40.000 ° - Step: 0.020 ° - Step time: 1.0 s - Tem

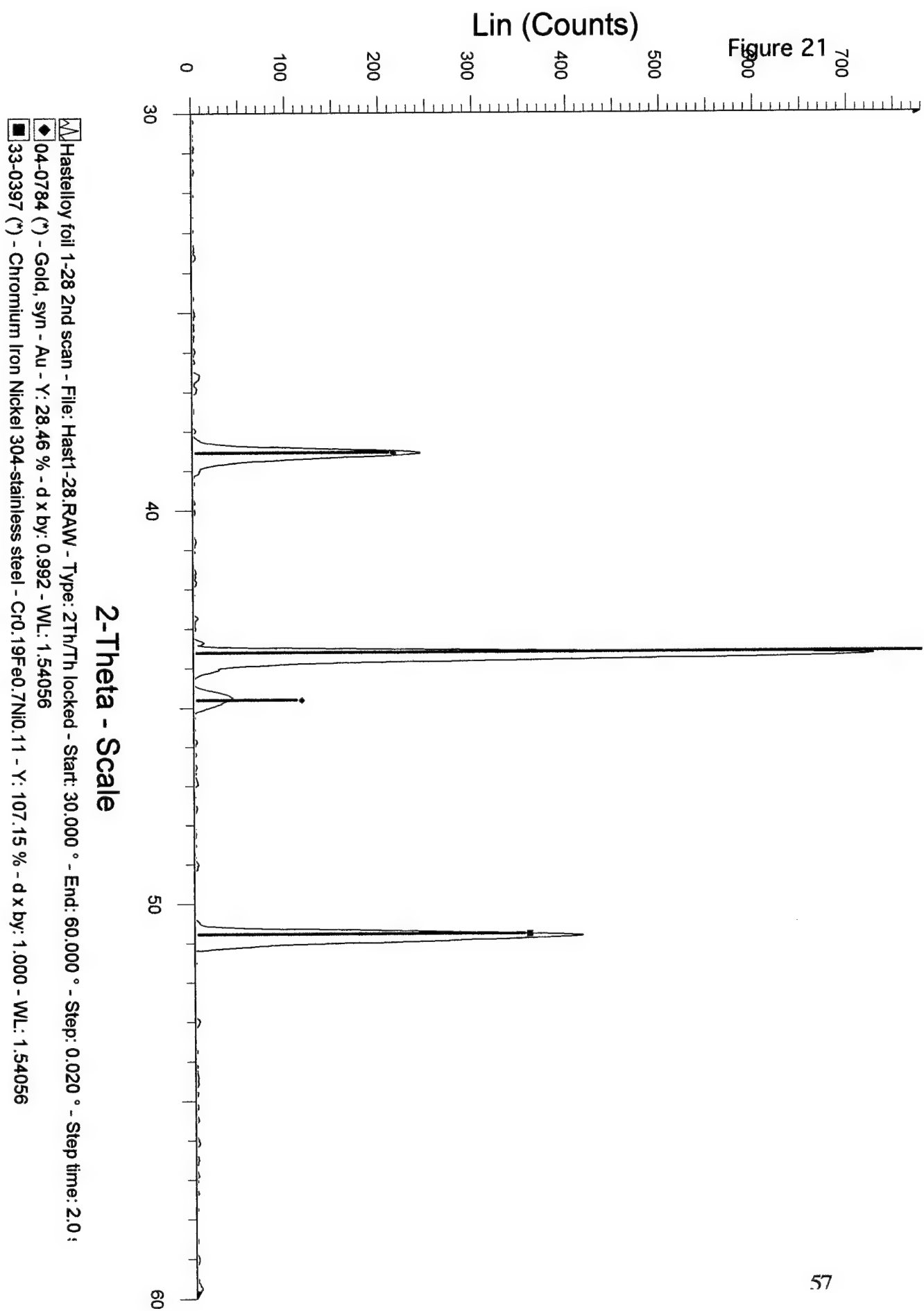21-1276 (*) - Rutile, syn - TiO2 - Y: 110.37 % - d x by: 1.000 - WL: 1.54056

d=2.4835

47

Figure 12

Figure 13

Figure 14

conc. Ti (ppm)

run time (hrs)

Ti - #1 conditions

Figure 15

51

solids from 1-6 Ti-Au expt - File: sol-1-6.RAW - Type: 2Th/Th locked - Start: 15.000 ° - End: 40.015 ° - Step: 0.005 ° - Step time: 1.0 s - T

21-1276 (*) - Rutile, syn - TiO2 - Y: 89.58 % - d x by: 1.000 - WL: 1.54056

04-0784 (*) - Gold, syn - Au - Y: 6.25 % - d x by: 1.000 - WL: 1.54056

21-1272 (*) - Anatase, syn - TiO2 - Y: 4.17 % - d x by: 1.000 - WL: 1.54056

Figure 16
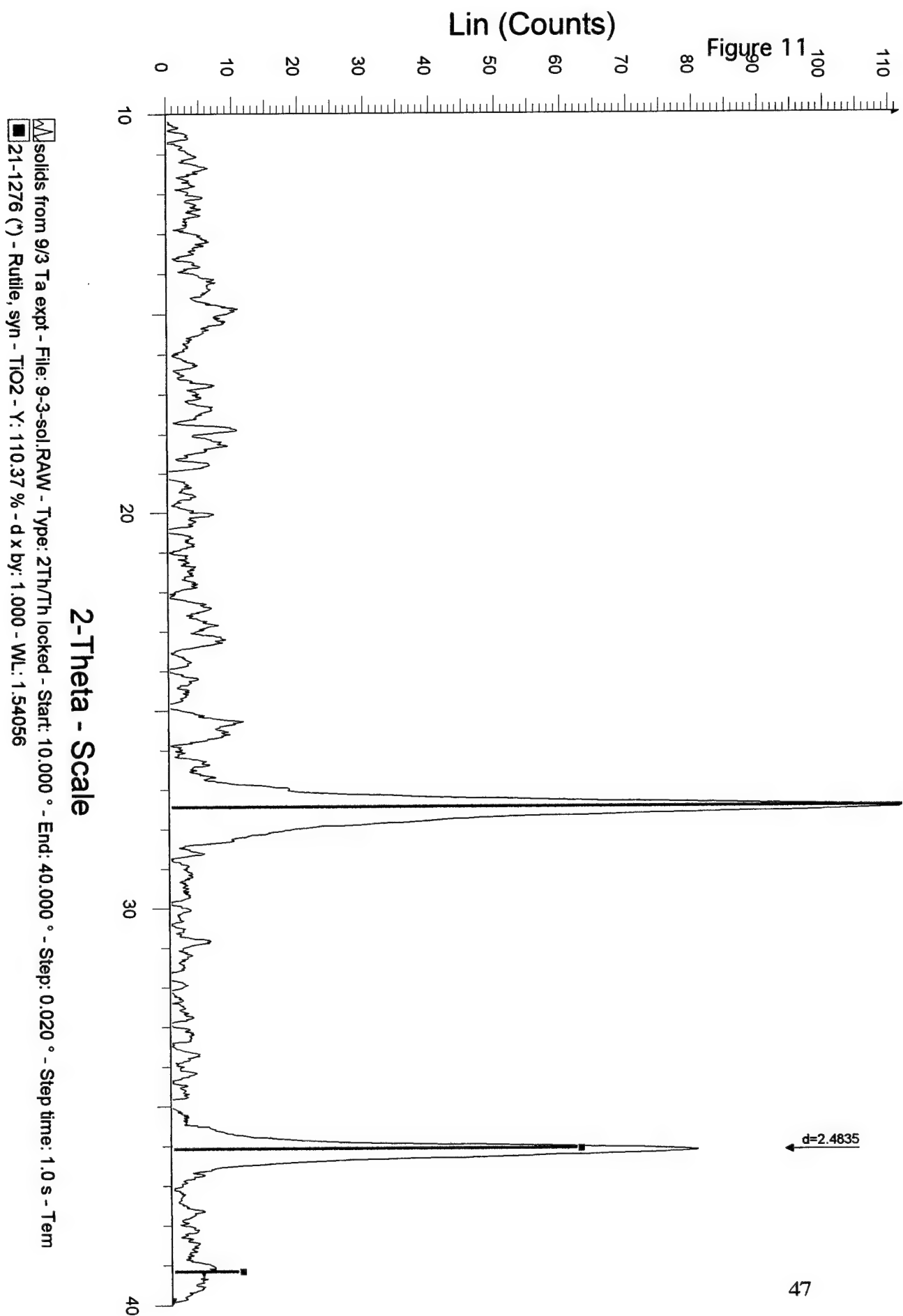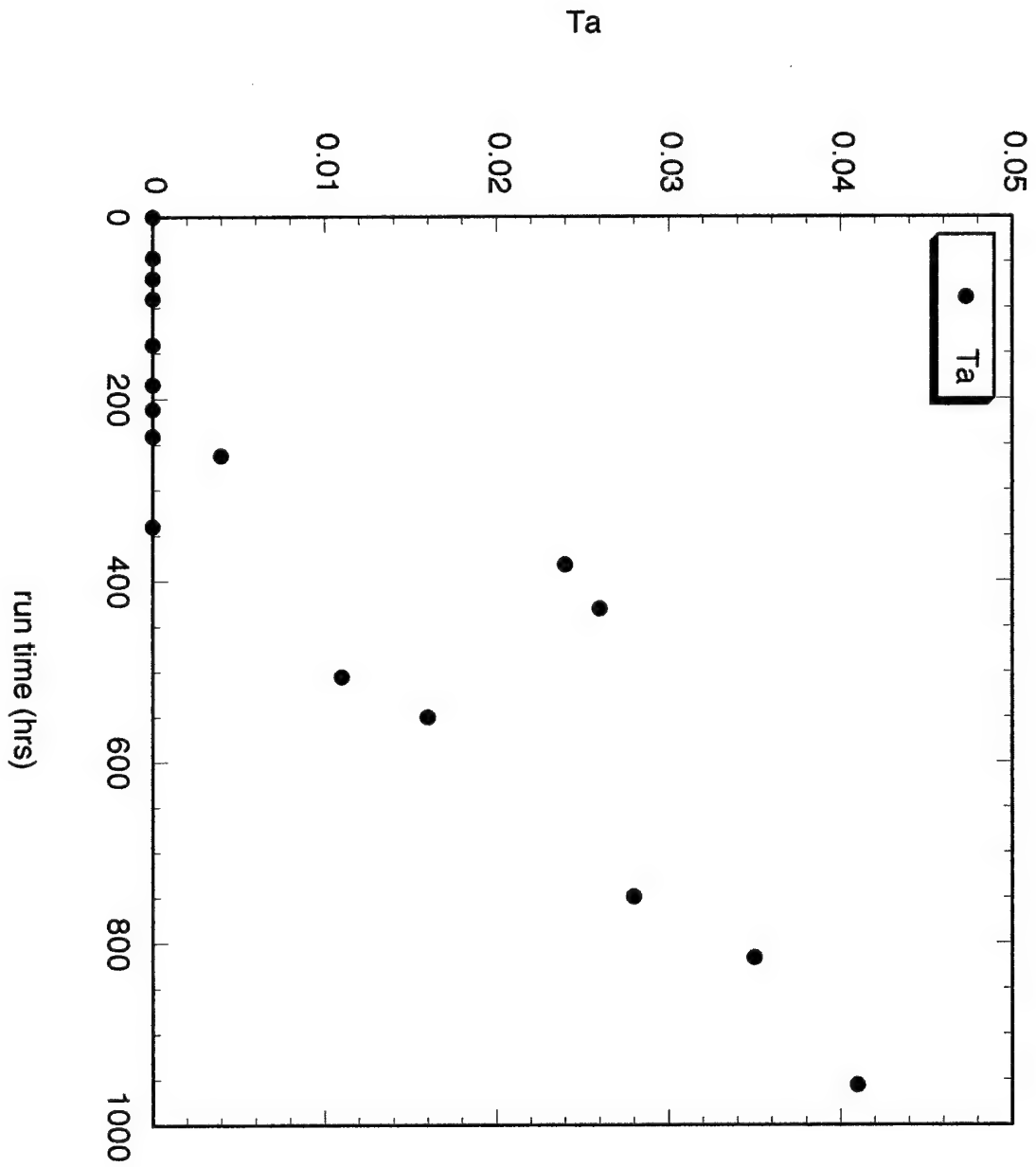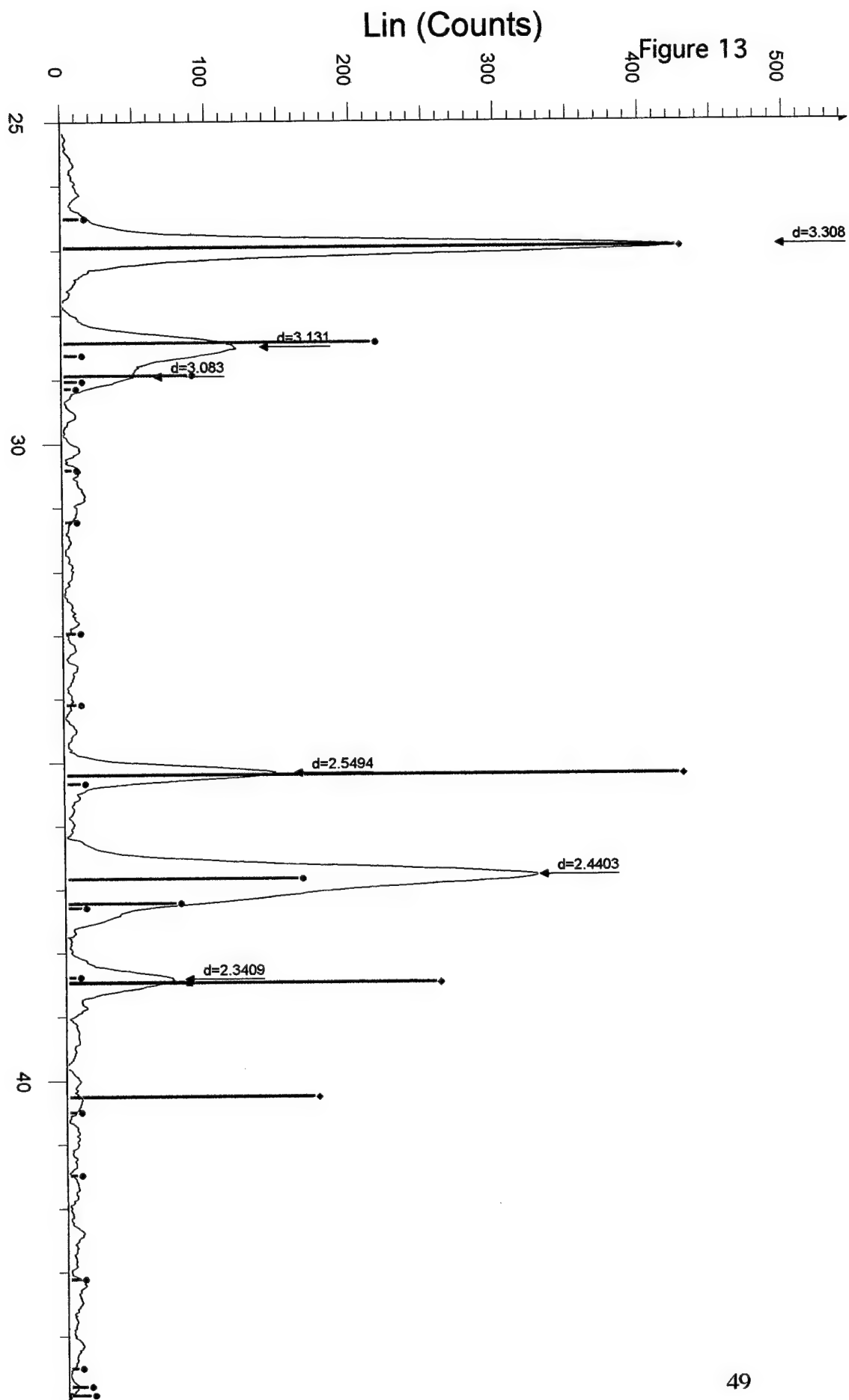
Line: composition of commercial 316SS
Points: metal content of experimental fluids,
recalculated to 100%

52

Figure 17

Figure 18

Figure 19

Figure 20

56

Figure 21

2-Theta - Scale

Lin (Counts)
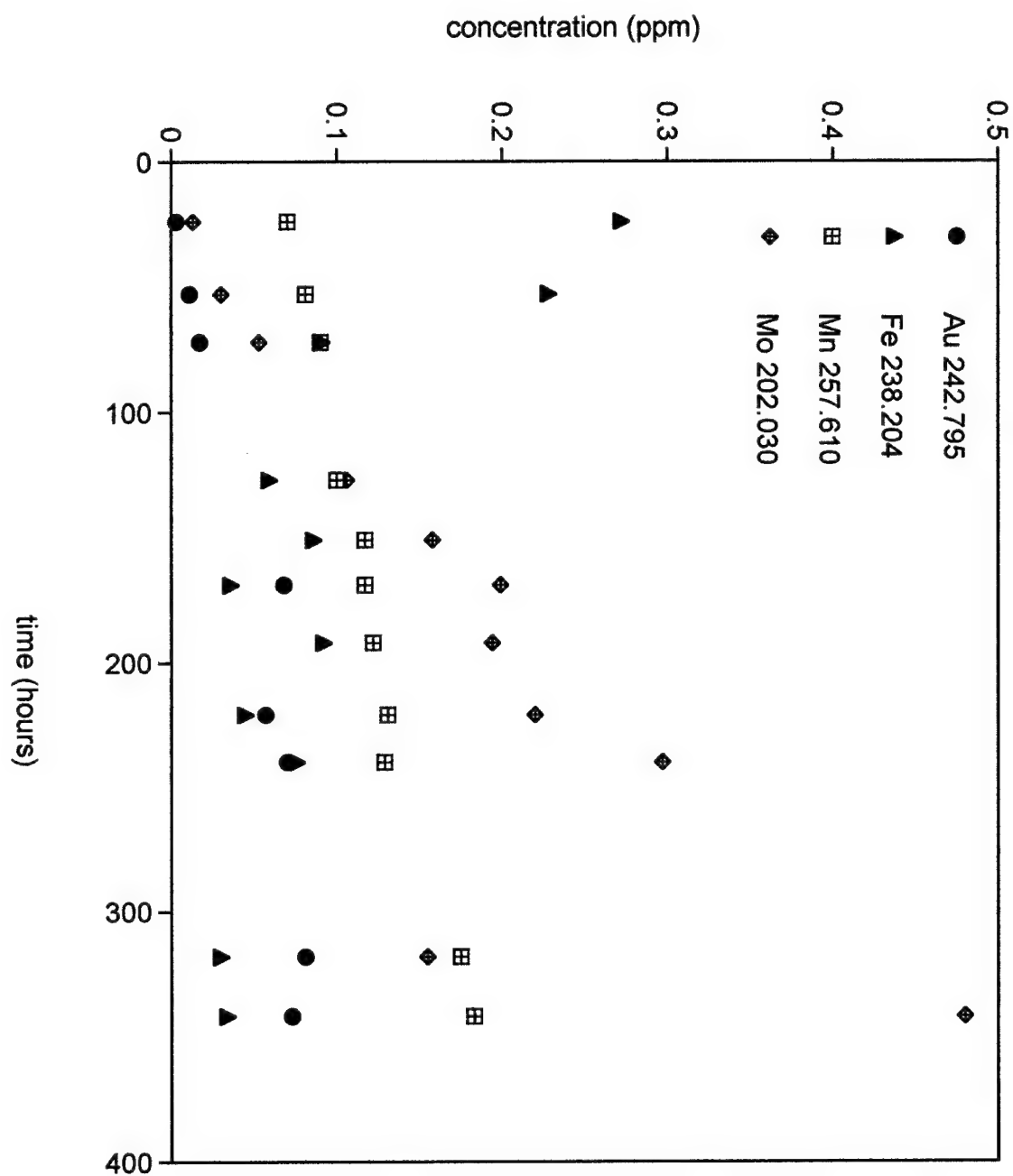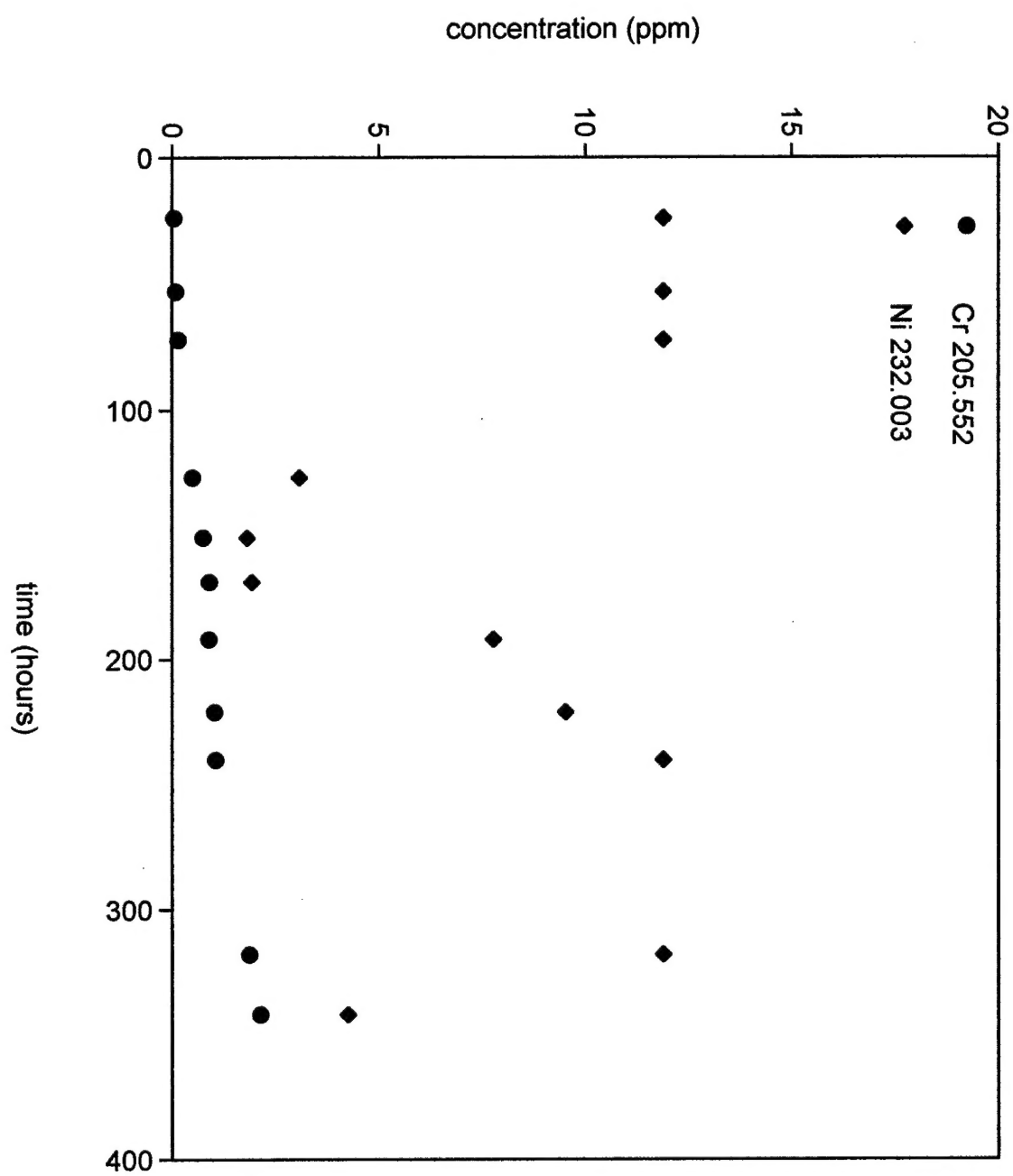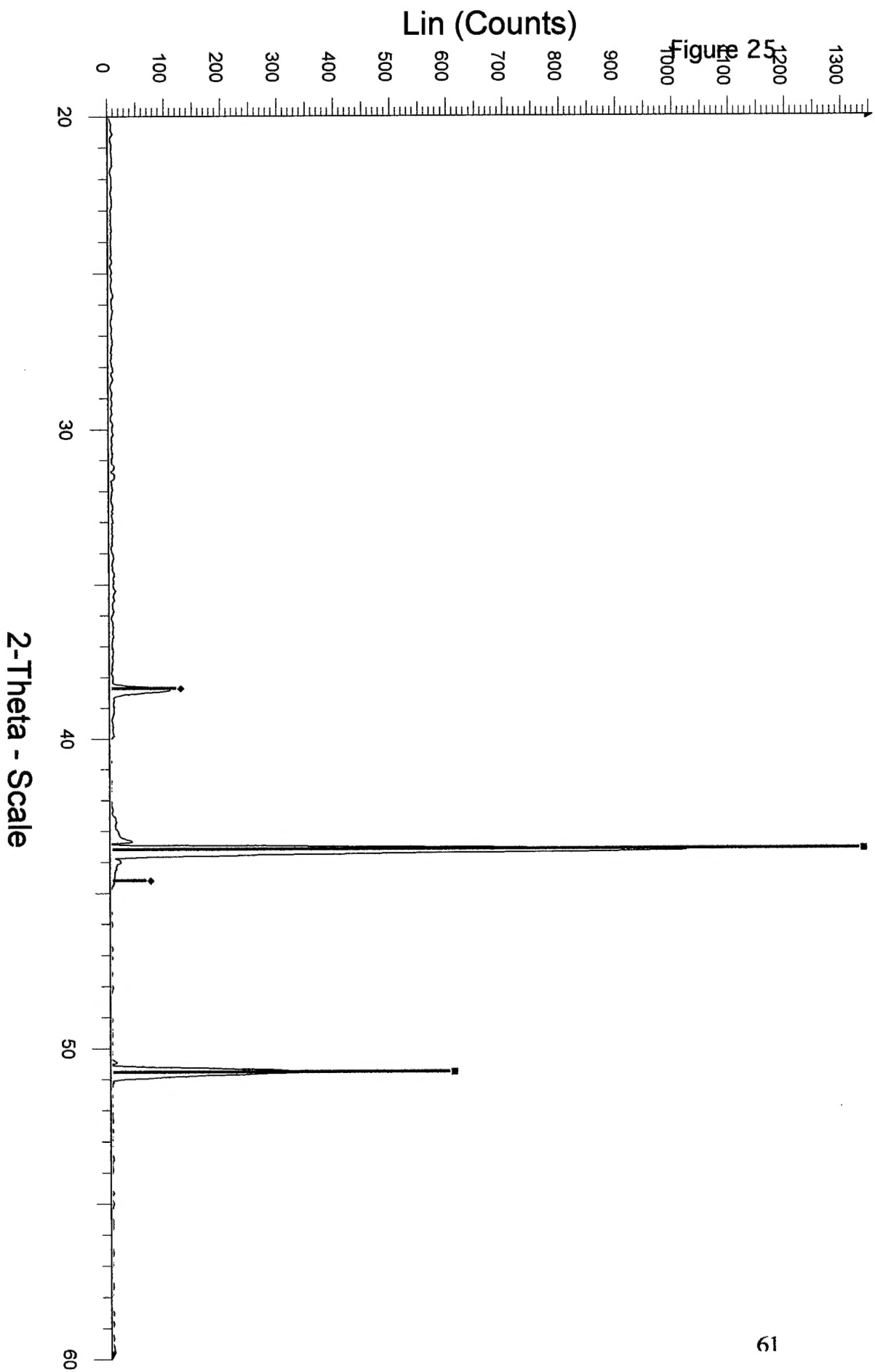
Hastelloy foil 1-28 2nd scan - File: Hast1-28.RAW - Type: 2Th/Th locked - Start: 30.000 ° - End: 60.000 ° - Step: 0.020 ° - Step time: 2.0 s
04-0784 (*) - Gold, syn - Au - Y: 28.46 % - d x by: 0.992 - WL: 1.54056
33-0397 (*) - Chromium Iron Nickel 304-stainless steel - Cr0.19Fe0.7Ni0.11 - Y: 107.15 % - d x by: 1.000 - WL: 1.54056

57

Figure 22

2-Theta - Scale

solids from 1/28/99 Hast expt - File: sol1-28.RAW - Type: 2Th/Th locked - Start: 20.000 ° - End: 50.000 ° - Step: 0.020 ° - Step time: 2.0 s
33-0664 (*) - Hematite, syn - Fe2O3 - Y: 100.00 % - d x by: 1.000 - WL: 1.54056
04-0784 (*) - Gold, syn - Au - Y: 8.33 % - d x by: 1.000 - WL: 1.54056

58

Figure 23

Figure 24

Figure 25

61

Figure 26

Figure 27